UNIVERSITÄTSKLINIKUM HAMBURG-EPPENDORF

Zentrum für Experimentelle Medizin
Institut für Klinische Pharmakologie und Toxikologie

Prof. Dr. med. Rainer H. Böger

Effect of nitroxyl in an *in vivo* mouse stroke model and in isolated healthy and atherosclerotic vessels

Dissertation

zur Erlangung des Grades eines Doktors der Medizin
an der Medizinischen Fakultät der Universität Hamburg.

vorgelegt von:

Gerryansjah Fischer
aus Hamburg

Hamburg 2017

Es irrt der Mensch, solang er strebt

Goethe 1808

Angenommen von der
Medizinischen Fakultät der Universität Hamburg am 20.03.2017

Veröffentlicht mit Genehmigung der
Medizinischen Fakultät der Universität Hamburg

Prüfungsausschuss, der Vorsitzende: Prof. Dr. med. Rainer H. Böger

Prüfungsausschuss, zweiter Gutacher: Prof. Dr. med. Karsten Sydow
Prüfungsausschuss, dritter Gutachter: Prof. Dr. med. Eike S. Debus

Contents

1 Introduction

1.1 The reduced form of nitric oxide: Nitroxyl

Nitric oxide (NO) is well recognized as an important modulator of vascular homeostasis with vasorelaxant, anti-aggregatory, and antiproliferative properties [1]. NO produced by NO synthase from the conversion of L-arginine to L-citrulline, activates the cytosolic enzyme soluble guanylyl cyclase (sGC) which catalysis the conversion of guanosine-5'-triphosphate (GTP) to cyclic guanosine monophosphate (cGMP) resulting in blood pressure regulation [2]. In addition to its vasoprotective effects, NO has been shown to be involved in neurotransmission [3], mitochondrial respiration [4], host defenses [5], and to possess antioxidant properties [6]. However, impairment of NO homeostasis is associated with a plethora of harmful effects in biological systems. Indeed, NO is involved in DNA strand breaks [7], tumor initiation/progression [8], protein/lipid oxidation [9], enzyme inhibition [10], deamination [11], and apoptosis [12]. Traditionally, it has been NO the main investigated nitrogen molecule. However, in the last years, a reduced form of NO such as nitroxyl (HNO/NO^-) has attracted scientific interest for its distinct chemical profile and biological effects from that of NO. These unique effects involving mainly the cerebro and cardiovascular systems have made nitroxyl a very promising pharmacological agent to be used under these diseases.

1.2 Chemistry of nitroxyl

Nitroxyl (HNO/NO^-) is the one-electron-reduced and protonated sibling of NO. Nitroxyl is considered to be one of the newest nitrogen species to be explored. It has been shown that the equilibrium constant *(*pK_a) of nitroxyl is 11.4, meaning that the predominant form at physiological pH levels is HNO rather than NO^- [13]. Quantum mechanical considerations support this observation. They show that the deprotonation of HNO is very slow due to the different energy states. Indeed, the ground state singlet electron configuration of ^1HNO is energetically more favorable than the ground state triplet of $^3NO^-$ [14] (Reaction 1).

$$^1HNO \rightarrow {}^3NO^- + H^+ \quad (1)$$

Therefore, the molecular form of nitroxyl in biological systems is accepted to be HNO. HNO has been shown to be remarkably reactive towards free thiols, thiol proteins and metal ions, while NO must first be activated to a more oxidized nitrogen oxide species [15]. Considering the high concentration of free thiols in cells (e.g. glutathione; GSH; 1-10 mM) and the high reactivity of HNO with thiols ($2\times10^6\ M^{-1}\ s^{-1}$) [16], it has been suggested that the scavenging of HNO by free thiols (and thus its inactivation) might be the predominant fate of HNO in

biological systems. However, several reports have shown that selected thiol proteins can be substantially inhibited at very low HNO levels without altering free thiol concentrations [16-17], offering to HNO the potential to have biological effects. The reaction of HNO with thiols can have at least two possible outcomes depending on the reaction conditions [18]. In a first step, this reaction leads to the formation of an intermediate N-hydroxy-sulfenamide (R-S-NHOH). In the presence of additional thiols (or vicinal thiols), a further reaction occurs resulting in the corresponding disulfide (R´SSR) and hydroxylamine (NH_2OH; Reaction 2). In the absence of additional thiols, a rearrangement occurs giving a sulfinamide species ($R\text{-}SNH_2{=}O$) (Reaction 3).

$$R\text{-}SH + HNO \rightarrow R\text{-}S\text{-}NHOH \rightarrow R'SSR + NH_2OH \quad (2)$$

$$R\text{-}S\text{-}NHOH \rightarrow R\text{-}SNH_2{=}O \quad (3)$$

These thiol reactions have aroused great interest because they may act as a redox on/off switch for enzymes containing cysteine residues. A screening of the entire proteome has identified several proteins that are targeted by HNO [19] (See Table 1).

Protein	Function	Modification	Effect
GAPDH	Glycolysis	Cys-152/156: SS-Bond Cys-247: Sulfonamide	Inhibition
Cathepsin B	Lysosomal protease	Active center cysteine: Probably sulfinamide	Inhibition
NMDA receptor	Calcium flux regulation	Probably S-S bond	Inhibition
Complex II	Oxidative phosphorylation	Probably S-S bond	Inhibition
Ryanodine receptor 1 and 2	ER calcium channel	Probably S-S bond	Activation
SERCA	ER calcium pump	Cysteine 674 + GSH: SS-bond	Activation
Soluble guanylate cyclase	cGMP synthesis		Activation
Transient receptor potential channel 1	CGRP release	Cys-665/651	Activation

Table 1: HNO-modified proteins, ER=endoplasmic reticulum

Besides reactions with thiols and thiol proteins, HNO interacts with metalloproteins [16, 20]. The reaction of HNO with ferrous heme proteins leads to the formation of a ferrous–HNO complex (Reaction 4),

$$Me^{2+}\text{ (heme)} + HNO \rightarrow Me^{2+}\text{-N(H)O (heme)} \quad (4)$$

while the reaction of HNO with ferric heme proteins such as myoglobin generates the corresponding ferrous-NO complex in a process referred to as reductive nitrosylation (Reaction 5).

$$Me^{3+}\text{ (heme)} + HNO \rightarrow Me^{2+}\text{-NO (heme)} + H \quad (5)$$

The reaction of HNO with metalloproteins is generally considered to be weak [21] giving HNO the possibility of escaping from the heme pocket of the protein and reacting with other molecules [22].

Therefore, the major known biological targets of HNO are thiols, thiol proteins and metalloproteins, and this offers the possibility to HNO to have biological relevance. However, whether HNO is an endogenously generated species is still under debate due to the lack of direct and sensitive detection methods. The likelihood of the endogenous generation of HNO is described below.

1.3 Does nitroxyl exist as an endogenously generated species?

Several reports in the HNO field have addressed the concept of putative endogenous HNO formation from NO synthase (NOS)-dependent and -independent sources in the myocardium [23], vasculature [24], and brain [25]. NOS works by converting L-arginine to NO and L-citrulline, and consumes in this process O_2 and NADPH while utilizing the cofactor tetrahydrobiopterin (BH_4). However, when NOS is in its uncoupled state (induced by the absence of either arginine or BH_4), it also produces N-hydroxy-L-arginine (NOHA), as well as peroxide and superoxide. Under these conditions, HNO is formed by the direct oxidation of NOHA [26] or by the catalysis of arginine to citrulline [27]. In addition to these NOS-dependent mechanisms, there are also a number of possibilities for NOS-independent formation of HNO. Mechanisms involving the decomposition of nitrosothiols [18], the dismutation of NO into HNO [28], the reduction of NO by xanthine oxidase [29], and the oxidation of hydroxylamine have also been described [30].

Recently, Filipovic's group provides evidence of endogenous HNO production and subsequent activation of a neuroendocrine signalling pathway regulating the vascular tone.

These authors have found that HNO is generated by the reaction of NO and hydrogen sulfide followed by the direct activation of the transient receptor potential channel A1 via the formation of disulfide bonds with cysteine residues in the receptor, resulting in a release of calcitonin gene related peptide (CGRP) [31].

Altogether, there is a high possibility for HNO to be an endogenous generated molecule. However, this point is still under debate due to the lack of direct and sensitive detection methods and remains the main challenge for the HNO field. Independent of HNO being an endogenous generated molecule, exogenous HNO has been shown to have important biological effects [32]. In these studies the use of HNO donors was necessary due to the high HNO reactivity. There are many HNO donors available [33]. However, only few of them are suitable for *in vivo* or even *in vitro* studies. In the present thesis, I used Angeli's salt ($Na_2N_2O_3$; AS) or 1-nitrosocyclohexyl acetate (NCA) as HNO donors. AS is a very established HNO donor but, due to its chemistry, cannot be used for *in vivo* studies. NCA is a new HNO donor with high potential for in vivo applications. Both HNO donors are described below.

1.4 Nitroxyl donors

HNO reacts with itself to form an intermediate dimer which decomposes into water (H_2O) and nitrous oxide (N_2O, reaction 6 [34]). The high reactivity of HNO precludes its storage; hence it is necessary to use an HNO donor in chemical and, especially, in biological studies.

$$HNO + HNO \rightarrow HON{=}NOH \rightarrow N_2O + H_2O \quad (6)$$

The most frequently used HNO donor is Angeli's salt ($Na_2N_2O_3$; AS). AS was synthesized 100 years ago by the Italian chemist Angelo Angeli [35]. It is commercially available with a guaranteed grade of purity. AS is stable in basic solutions which may cause pH rearrangements, and it has a half-life of 2.5 min at physiological pH ranges (4-8) [36].

Unfortunately, decomposition of AS results not only in HNO but also in the formation of one equivalent nitrite ion (NO^{2-}) (Reaction 7), which possesses biological activity [37].

$$N_2O_3^{2-} + H^+ \rightarrow HNO + NO^{2-} \quad (7)$$

To overcome AS limitations, co-release of NO^{2-} and short half-life, the HNO donor 1-nitrosocyclohexyl acetate (NCA) was synthesized by King's group [38] which possess different chemical properties than AS. NCA belongs to the acyloxy nitroso compounds that generate HNO and the corresponding ketone upon hydrolysis in aqueous solutions in a pH-dependent manner as follows (Reaction 8).

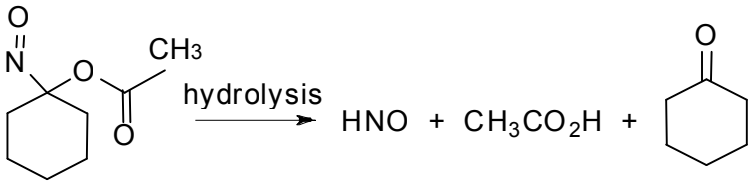

(8)

NCA is a bright blue liquid at room temperature with strong UV-vis absorption at 667 nm, ε = 20.7 M^{-1} cm^{-1} and IR absorption for the carbonyl (1750 cm^{-1}) and nitroso groups ($\nu_{N=O}$ = 1561 cm^{-1}) [38]. NCA releases very low amounts of NO (less than 1%) and total nitrate/nitrite (3-4%). The kinetics, products, and the mechanism of HNO released from NCA have been recently reported [39]. NCA is a long-lasting HNO donor as it hydrolyzes slowly (half-life = 800-890 min) under neutral buffer conditions [38].

The properties of the two HNO donors described above are summarized in Table 2.

HNO donor	Structure	By-products	Half-life at pH7
Angeli's salt ($Na_2N_2O_3$)	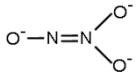	Nitrite anion (NO_2-)	2.3 min
1-Nitrosocyclo-hexyl acetate (NCA)	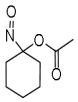	Cyclohexanone, acetic acid	>3 h

Table 2: The structure and chemical properties of NCA compared to Angeli's salt

In the present thesis, we have used these donors to investigate the effect of HNO in an *in vivo* mouse stroke model, and the mechanism of action of HNO-induced vasorelaxation in healthy mice and in a mouse model of atherosclerosis.

1.5 Ischemic stroke

According to the Federal Statistical Office, stroke was the most frequent cause of death in Germany in 2014, costing a total of 16,753 lives. It is the most frequently reason for becoming severely disabled [40], [41]. The life-time cost per year has been calculated as 43,000 € [42]. This highlights the importance of this disease for the scientific and health community. In addition, it is a fateful event for the person concerned as well as for his or her relatives.

The formation of an ischemic stroke thrombus (a mass of aggregated platelets resting at the place of origin) or an embolism (an embolus consisting of thrombocytes which, after being

transferred by the bloodstream, settle at a site far from their origin) leads to a decrease in the blood flow behind the bottleneck, and therefore in a reduced supply of nutrients to the neuronal tissue. This leads to three main harmful conditions as shown in Figure 1: (1) depletion of adenosine triphosphate (ATP); (2) failure of glutamate homeostasis; and (3) formation of free radicals, especially reactive oxygen species (ROS) [43].

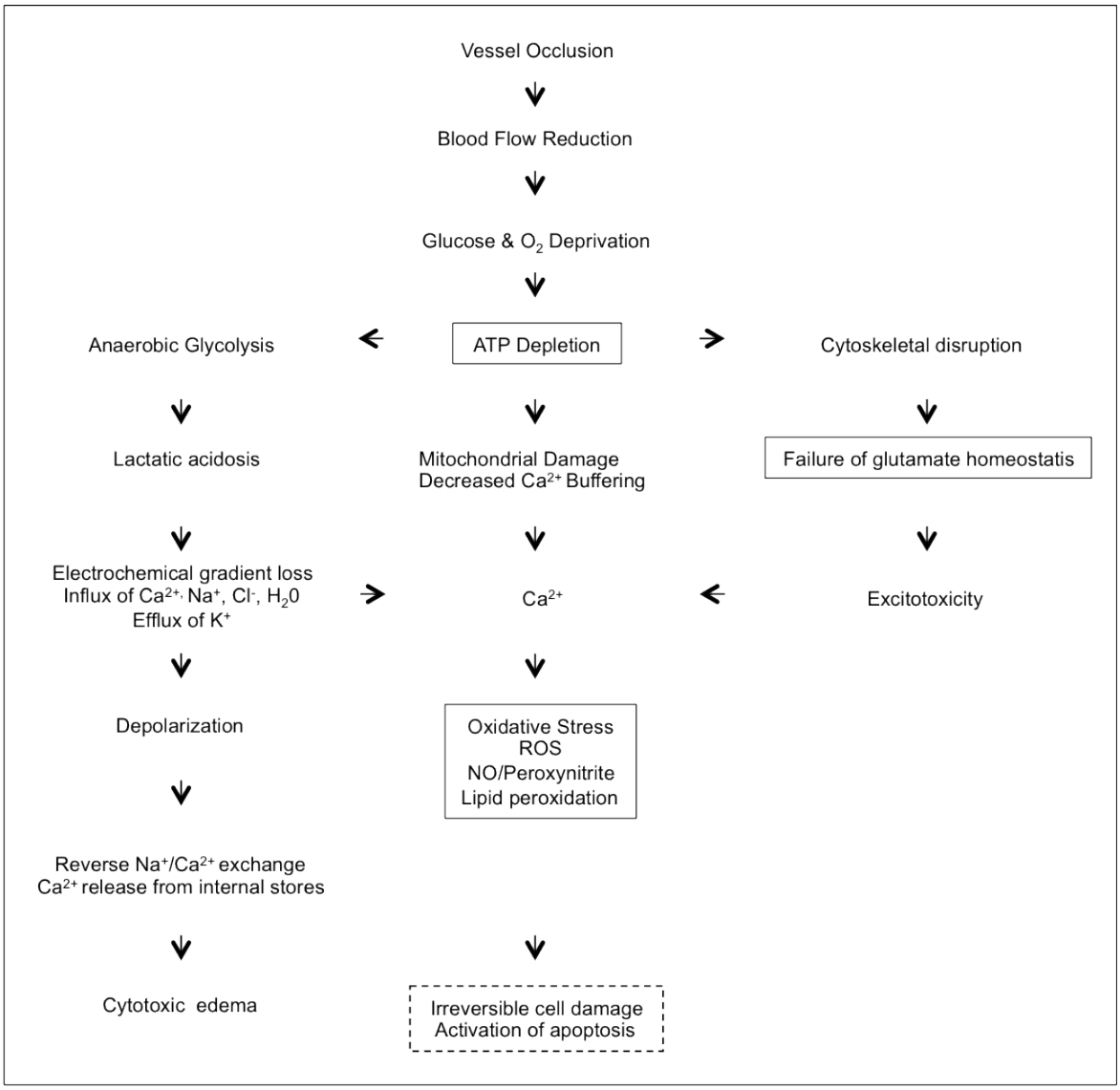

Figure 1: Synopsis of mechanisms in ischemic stroke [45], modified.

The inadequate supply of oxygen and glucose to the brain is critical to neurons, as their ability to tolerate it is very limited. Indeed, most neurons are not able to store oxygen (in neuroglobins) or glucose (in the form of glycogen) [44]. It is widely accepted that a breakdown in the respiratory chain leads to a rapidly used ATP. Only 15 s of ischemia are followed by the total consumption of ATP. This lack of energetic phosphates leads to a decreased activity of ATP-dependent membrane ion pumps and hence a progressive collapse of the membrane

potential. This is initially followed by a loss of electrical activity (neuronal signal transmission) and then by a loss of structure (membrane integrity) [45].

Table 3 shows the level of cerebral blood flow and its influence on the functionality of neurons [46].

CBF situation	CBF [mL/g/min]	Protective mechanism	Electrical activity	Membrane integrity
Normal	~ 0.50	Autoregulation	++	++
Reduced compensated	~ 0.35-0.45	Anaerobic glycolyse	++	++
Reduced	~ 0.20-0.35	Reduced metabolism	+	+
Markly reduced	~ 0.10-0.20	-	-	+
Severly reduced	< 0.10	-	-	-

Table 3: Cerebral blood flow and its influence on the functionality of neurons [Hamann 1997, modified]

The direct consequence of a loss of neuron structure is an uncontrolled release of the excitatory neurotransmitter glutamate and a lack of its uptake [47]. The elevated glutamate concentration leads to an uncontrolled overstimulation of N-Methyl-D-aspartate (NMDA) receptors [48] and subsequently to a dramatic increase in intracellular Ca^{2+} concentration [49]. Glutamate-induced calcium inflow is followed by the induction of apoptotic signal cascades. These mechanisms are amplified by the formation of free radicals, such as reactive oxygen (ROS) or nitrogen (RNS) species which are able to affect DNA or biological membranes via lipid peroxidation [50]. However, in areas where perfusion is partially maintained through the vasodilation of patent vessels and blood supply from collaterals, the tissue is electrically hypoactive but structurally still intact and viable. This tissue surrounding the ischemic core is referred to as the penumbra [51].

1.6 Oxidative stress in ischemic stroke

As mentioned above, ROS and RNS accumulation plays an important role in damaging biological membranes via lipid peroxidation in pathological conditions like ischemic stroke. ROS are inherently unstable molecule, therefore biomarkers are necessary for measuring oxidative stress load [52]. Isoprostanes (prostaglandin-like compounds) detection and quantification are mostly used as marker of oxidative stress. Isoprostanes formation is observed in the non-enzymatic lipid peroxidation of arachidonic acid as shown in Figure 2.

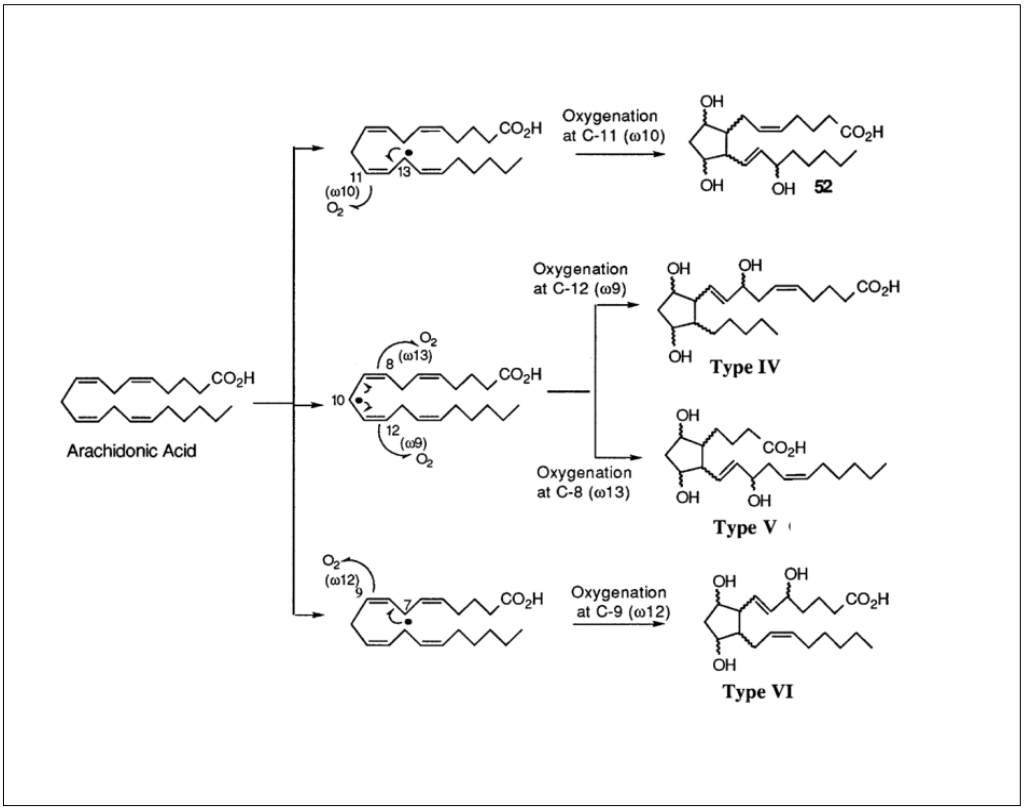

Figure 2: Formation of different groups of isoprostanes [53] modified.

Isoprostanes, as end product of that oxidation, are stable and can be quantified in biological tissues and liquids [54].

1.7 Nitroxyl and neuroprotection *in vitro*

HNO has been shown to regulate protein function through covalent modification of thiol groups on protein cysteine residues [55], [56], [57]. The NMDA receptor is one of these proteins which structure and consequently function is altered by HNO. The NMDA receptor possesses a redox modulatory site which consists of critical cysteine residues. It has been shown that reduced cysteine residues led to an increase in the magnitude of NMDA-evoked responses while oxidized cysteine residues led to a decrease of NMDA effects [58]. Many i*n vitro* studies have demonstrated that HNO is able to modulate NMDA receptor activity. In particular, HNO reacts directly with Cystein-399 in the NR2A subunit of the NMDA receptor to downregulate excessive NMDA-evoked responses and subsequent excessive Ca^{2+} influx [59], [47], [58], [60]. These effects of HNO showed *in vitro* neuroprotection against increased intracellular Ca^{2+} levels [59]. In addition to the modulatory effect of NMDA receptors, HNO has been shown to directly decrease ROS levels through its antioxidant function during lipid peroxidation, also leading to neuronal protection [61]. Therefore, the ability of HNO to modulate NMDA receptor activity *in vitro*, in parallel with its ability to interact and scavenger ROS, led us to hypothesize that HNO effects could apply as well to an *in vivo* system. Therefore, our

main focus was the translation of the *in vitro* function of HNO on NMDA receptor to an *in vivo* mouse-stroke model, in which stroke was induced by middle cerebral arterial occlusion (MCAO). In particular, I quantified the levels of ROS in mice subjected to MCAO intervention in presence of HNO treatment or to vehicle.

1.8 Hypertension and atherosclerosis

In 2014, the Federal Statistical Office considered death from five manifestations of cardiovascular disease to be among the ten most frequent causes of death in Germany, leading to a total of 338,056 deaths. In 2013, the overall healthcare expenditure in Germany was about 315 billion €. Of this, 44 billion € (14 %) were spent in connection with cardiovascular diseases proving how prominent are such diseases for the health community.
The underlying cause of cardiovascular diseases is atherosclerosis, while the main risk factors are hypertension, cigarette smoke, diabetes and elevated plasma levels of low-density lipoprotein (LDL). Hypertension leads to small endothelial lesions as well as disruptions in the endothelial repair process. This attracts pro-inflammatory monocytes to invade the space between intima and media. Cigarette smoke (probably by boosting ROS formation) and diabetes (probably via the glycosylation of critical proteins) amplify this process. In the next step, monocytes are transformed into macrophages by expressing an LDL scavenger receptor. Fatefully, it is not possible for the macrophages to down-regulate the expression of LDL receptors, and thus they become foam cells prior to undergoing apoptosis. The accumulation of this necrotic material is called a stable atherosclerotic plaque. Under certain conditions, stable plaques become unstable, leading to disruption followed by embolism. These conditions lead to a cardiovascular event [62]. A synopsis of the underlying pathogenesis is given in Figure 3.

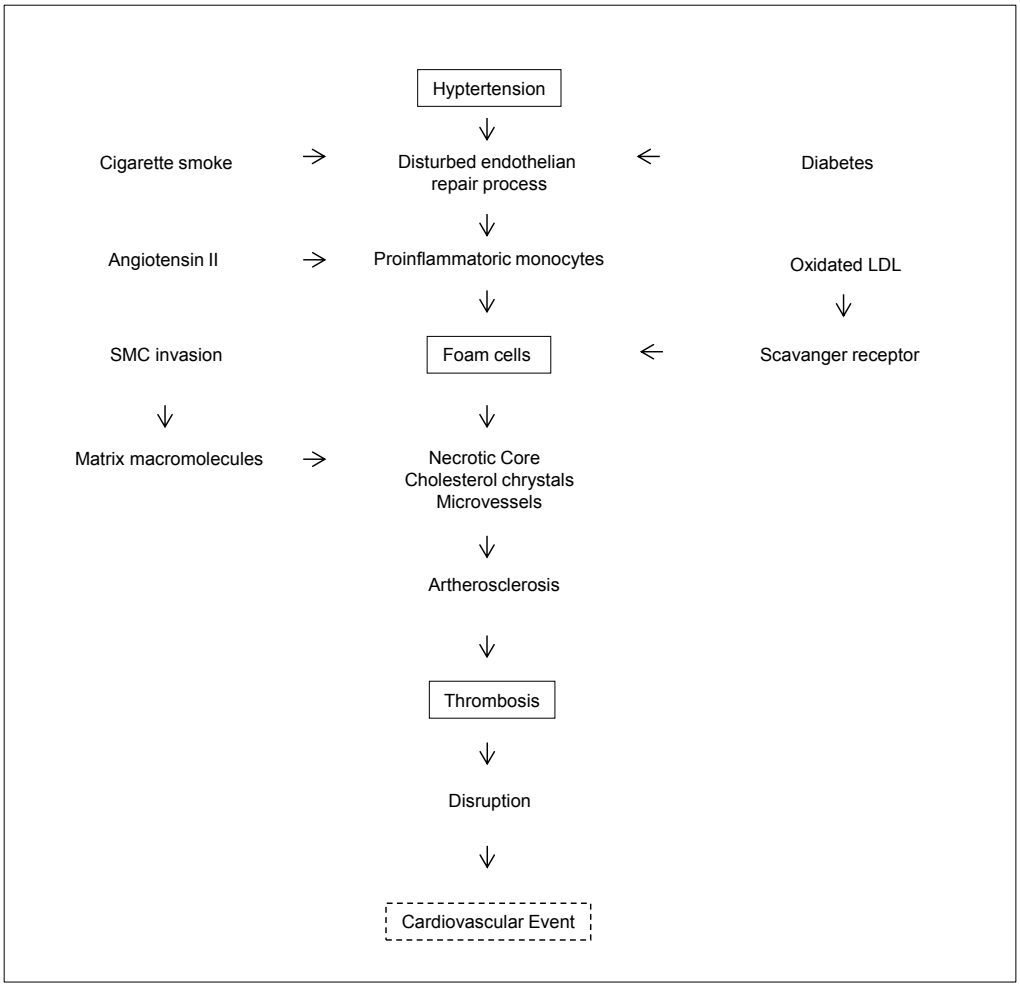

Figure 3: Synopsis of the pathogenesis of a cardiovascular event

Thus, hypertension is a crucial factor in the development of cardiovascular diseases, confirmed also in a large study [63]. Based on the results of several randomized controlled trials, treatment of – isolated systolic as well as diastolic – hypertension significantly improves the outcome of the treated group [64], [65]. Despite our knowledge about the substantial influence of life-style changes in reducing hypertension, pharmacological treatment has unfortunately become ever more prominent. Complex medical and even interventional therapeutic or device-based regimes are considered when treating hypertension [66].

1.9 Nitroxyl in the healthy vascular system

In clinic, the current therapeutic interventions to treat chronic hypertension are nitrovasodilators such as glyceryl trinitrate (GTN). However, treatment of patients with GTN leads to the well-recognized tolerance phenomenon, a condition in which the vasodilatory effectiveness of GTN is reduced after long-term use. This phenomenon of tolerance development might be attributed to the inactivation of NO, released from GTN, by ROS.

Like NO, exogenous HNO has been shown to be a potent vasodilator of both large conduit [26], [67] and small resistance arteries [68], and to possess anti-aggregatory [69], and anti-proliferative properties [70]. Importantly, in contrast to NO, HNO offers several advantages for potential therapeutic use. HNO maintains its vasoprotective actions also in spontaneously hypertensive rats [71], it is resistant to inactivation by ROS [72], its application in animal models does not result in vascular tolerance neither acutely *in vitro* [73] nor chronically *in vivo* [74], and HNO treatment does not induce cross-tolerance development resulting in a sustained vasodilatory effect in animals rendered tolerant to nitrovasodilators [73], [74]. These advantages of HNO could be of relevance in a clinical setting, making HNO a promising candidate as a novel therapeutic addition for treatment of vascular pathologies such as atherosclerosis.
However, the signaling pathway by which HNO elicits vasorelaxation is still unclear [75], [76]. One group has suggested that the vascular effects of HNO are, at least in part, mediated by increased circulating levels of calcitonin gene-related peptide [75], one of the most potent vasodilators known to date and thought to be involved in the regulation of coronary and brain circulation [77], [78], [79]. Others have suggested that the HNO-induced vasorelaxation is mediated by sGC, comparable to the effect of NO [75, 76]. Therefore, before promoting HNO as a novel and innovative therapeutic intervention, it was necessary to gain understanding of its exact mechanism of action and molecular targets in the vascular system.

1.10 Objectives

The goal of the present thesis was to quantify the levels of oxidative stress biomarkers and variation in blood pressure in a mouse-stroke model after exogenous application of HNO, and to understand the mechanism of how HNO elicits vasorelaxation in healthy and in mice subjected to atherosclerosis. To address these questions two specific aims per part were pursued:

Effect of nitroxyl in an *in vivo* mouse-stroke model

We quantified the effects of exogenous HNO on reactive oxygen species (ROS) levels in an *in vivo* mouse-stroke model. ROS biomarkers such as F_2-isoprostanes 8-iso-PGF2α in urine and F_2-isoprostane iPF2α-VI in blood were analyzed and quantified by gas chromatography mass spectrometry (GC-MS) and enzyme-linked immunosorbent assay (ELISA), respectively.

In addition, we measured systolic blood pressure in healthy mice and mice subjected to stroke after exogenous injection of HNO by tail-cuff plethysmography.

Effect of nitroxyl in isolated healthy and atherosclerotic vessels

We investigated the mechanism of how HNO elicits vasorelaxation in large arteries, in healthy and vascular-diseased mice. Aortic rings from wild-type (WT) mice were isolated and mounted in an organ bath system. The vessels were treated with several pharmacological inhibitors of important pathways potentially involved in HNO-mediated vasorelaxation.

Mice deficient in apolipoprotein E ($ApoE^{-/-}$) were chosen as mouse model of atherosclerosis.

2 Materials and Methods

2.1 Middle brain artery occlusion

Middle brain artery occlusion (MCAO) was chosen as an *in vivo* mouse-stroke model [80]. C57BL/6 male mice (12–15 weeks old) were anesthetized with 3–4% isoflurane during initial induction and 1.5–2% during surgery, achieved by passing 100% oxygen (0.4–0.5 L/min) through an isoflurane vaporizer set. After the initial induction, mice were injected intraperitoneally with buprenorphine (0.05 g/kg) and 100 µL of either Angeli´s salt as HNO donor (AS, 40 µmol/kg, neutralized to pH 7 with HCl) or 0.9% NaCl as control. Temporary occlusion of the middle cerebral artery was then initiated using the intraluminal filament method (6–0 nylon) as previously described [80]. Briefly, the left common and external carotid arteries were isolated and ligated (5–0 silk). A monofilament (6–0 nylon, blunted 0.22–0.24 mm) was inserted into the external carotid artery and advanced into the middle cerebral artery until light resistance was felt (roughly 9 mm). The filament was removed after 1 h.

The surgical procedure as well as sample collection via metabolic cages was performed by Dr. med. Chi-un Choe, Department of Neurology, University Medical Center Hamburg-Eppendorf (UKE). In addition, his team assessed the neurological clinical outcome of the mice and measured the histological infarct size.

2.2 Measurement of systolic blood pressure

Non-invasively measurement of systolic blood pressure by tail-cuff plethysmography (TSE 209000; TSE Systems, Bad Homburg, Germany) was used as previously described [81,82]. C57BL/6 male mice (13-15 weeks) were placed in a tube and the last third of tail was placed between a lamp and a photocell. The first third of tail was surrounded by a pressure cuff. The recorded data were amplified and visualized using an oscilloscope. Blood pressure was measured immediately and 30 min after i.p. injection (100 µL) of either AS (40 µM/kg, neutralized to pH 7 with hydrogen chloride; HCl) or 0.9 % NaCl.

2.3 Measurement of F_2-isoprostane 8-iso-PGF2α

Twenty-four hours after MCAO induction, urine was collected over a period of 6 h in specially designed metabolic cages and stored at -20°C until analysis. Prior to purification and derivatization, the samples were defrosted overnight at 4°C. Part of each sample (50 µL) was retained for further measurement of creatinine. Thus, 200 µL of urine were diluted with 800 µL ultrapure water, and 1 ng/mL of a stable isotope internal standard 16,17,18,19-[$_2H^4$]-iP$F_{2\alpha}$-

III (Cayman Chemical, Tallinn, Estonia) was added into the sample. The purification of the samples was performed using a 5 mL immunoaffinity column coated with antibodies directed against F_2-isoprostanes 8-iso-PGF2α (Cayman Chemical, Michigan, USA) as described elsewhere [54]. Before use, the columns were washed twice with a 0.1M phosphate buffer prepared by combining 13.3 g dipotassium phosphate (K_2HPO_4), 32.22 g potassium dihydrogen phosphate (KH_2PO_4), 0.5 g sodium azide (NaN_3), and 29.2 g sodium chloride (NaCl) diluted to 1.0 L with ultrapure water at pH 7.4. Thereafter, the whole sample was allowed to pass through the column followed by 2 mL of ultrapure water. After adding 2 mL of ethanol (C_2H_5OH, 95 % (v/v)) into the column, the throughput under the column was collected. Subsequently ethanol was evaporated under a stream of dry nitrogen (N_2). Sample derivatization was achieved as previously described [83]. For the first derivatization, the residue was dissolved in a mixture of 100 µL acetonitrile (CH_3CN), 10 µL methanol (CH_4O), 10 µL *N*,*N*-diisopropylethylamine ($C_8H_{19}N$) and 10 µL 2,3,4,5,6- pentafluorobenzyl bromide (PFB) 33 % (v/v) in CH_3CN. After 1 h incubation at 30°C, samples were again evaporated under a stream of dry nitrogen. For the second derivatization, the residue was dissolved in 100 µL of N,O-bis(trimethylsilyl) trifluoroacetamide (BSTFA) and incubated at 60 °C for 1 h. Thereafter, samples were dissolved in methanol and ready for GC-MS measurement.

GC-MS analyses were performed using a quadrupole mass spectrometer 1200 (Varian, Walnut Creek, USA) coupled with a gas chromatograph CP-3800 (Varian). The gaseous separation proceeded by means of a 30 m x 0.25 mm (length x diameter) FactorFour-5MS capillary column (Varian) with a film thickness of 0.25 µm. The following sequence of temperatures was chosen for the heating the capillary column: 70°C for 2 min, heating to 280°C at a rate of 25°C/min, heating to 325°C at a rate of 5°C/min. Helium was used as the carrier gas, with a constant flow of 1 mL/min. The temperature of the injector was 150°C at injection. Subsequently, it was immediately adjusted to 300°C at a rate of 100°C/min. The injection volume was 2.0 µL in the split/splitless mode. A 1:10 split was used at injection time and closed after 20 sec. The transfer line and the ion source were heated to a constant temperature of 300°C and 170°C respectively. Under the chosen negative ion chemical ionization conditions, the ionization energy was 70 eV and the electron current 160 µA. In the ion source, methane was used for chemical ionization. A voltage of 1.4 kV was applied to the electron-multiplier for detecting the ions. The concentration of F_2-isoprostanes 8-iso-PGF2α was normalized to urine creatinine to avoid the influence of the glomerular filtration rate.

The creatinine concentration was kindly analyzed by Dr. med. Haddad in the Department of Clinical Chemistry, UKE, using a Hitachi 917 analyzer equipped with a Roche Jaffe enzymatic creatinine assay.

2.4 Measurement of F_2-isoprostane iPF2α-VI

Two days after MCAO induction, the mice were killed and their blood was collected and stored at -80 °C until analysis. The plasma isoprostane F_2-isoprostane iPF2α-VI level was analyzed using an ELISA according to the manufacturer's instructions (Cayman Chemical Europe). Samples were thawed overnight at 4°C, centrifuged at 9200 g, and subsequently analyzed in triplicate (50 µL aliquots). One test tube of each triplicate was spiked with $iPF_{2\alpha}$ -VI 5 ng/mL. Then, each sample was dissolved in 150 µL of acetone, incubated for 5 min at 4 °C and centrifuged at 3000 g for 10 min. The supernatant was transferred to a clean tube and resuspended in 2 mL of extraction buffer (1 M monosodium citrate ($NaH_2C_6H_5O_7$), pH 4.0, containing 10 % sodium chloride). The samples were then incubated for 90 min at room temperature. After adding 5 mL of methylene chloride, the lower fraction was transferred to a clean test tube. Before resuspending each sample in 1 mL of enzyme immunoassay (EIA) buffer, aliquots were evaporated to dryness under a stream of dry nitrogen. Subsequently, samples were incubated for 90 min at room temperature and ready to use. One hundred microliters of bulk standard (F_2-isoprostane iPF2α-VI 50 ng/mL) were transferred into a tube followed by a serially logarithmical dilution of the standard by removing 300 µL from the first into the second tube and repeating this process in the following tubes. The samples were then added into a 96-well plate. After incubation of the plate for 18 hours at 4 °C, Ellman's reagent (5,5'-dithiobis-(2-nitrobenzoic acid)) [84] was reconstituted with 20 mL of ultrapure water. Subsequently, the wells were emptied five times with the resulting wash buffer. In order to develop the assay, 200 µL of Ellman's reagent were placed in each well. The plate was covered with plastic film and placed on an orbital shaker in the dark for 120 min. Measurement of optical density was performed using a microtiter plate well photometer at a wavelength of 410 nm. Plasma concentrations of F_2-isoprostane iPF2α-VI in pg/mL were calculated using a standard curve of authentic F_2-isoprostane iPF2α-VI ranging from 50 to 5000 pg/mL. Plasma concentrations of F_2-isoprostane iPF2α-VI determined in C57BL/6 mice were similar to levels previously reported in these mice [85].

2.5 Measurement of vascular tension

WT male C57BL/6 mice (12-15 weeks old) were used to investigate the mechanism of action of HNO-induced vasorelaxation. Animals were anesthetized with carbon dioxide (CO_2) and killed by decapitation. The thorax was opened and an intracardial injection of heparin (0.05 ml of 10,000 IU/ml stock solution = 500 IU) was carried out about 5-10 min prior to the experimental protocol. The thoracic aorta was removed immediately, carefully cleaned of fat and connective tissue, and then cut into 3-4 mm wide transverse rings. The rings were placed in modified Krebs solution at pH 7.4, 37 °C under a resting optimal tension of 1.1 g, and a mixture of 95 % O_2 and 5 % CO_2 was bubbled through the solution. Isometric tension

was recorded using a force displacement transducer (Ingenieurbüro Jäckel, Hanau, Germany). The aortic rings in the bath tubes were allowed to equilibrate for 45 min. To check the viability of the rings, the aortic rings were pre-constricted twice with potassium chloride (KCl, 2 M). To assess the maximum constriction of the vessels, we performed concentration-response curves to prostaglandin $F_{2\alpha}$ ($PGF_{2\alpha}$). From the curves obtained, $PGF_{2\alpha}$ 5 µM resulted in approximately 75-80% of the maximum $PGF_{2\alpha}$ constriction. Therefore, we used this $PGF_{2\alpha}$ concentration through all study. When the vasoconstriction curve of the rings reached the plateau phase of the submaximal tension, we applied NCA as HNO donor. A cumulative concentration-response curve of NCA from 80 pM to 80 µM was constructed and the tension was recorded. The percentage dilation was calculated when the vasodilator curve reached the plateau phase of minimum tension.

To examine the possible targets of HNO in the vasculature, aortic rings were pre-incubated for 30 min with various different inhibitors after being pre-constricted with $PGF_{2\alpha}$. Only one inhibitor was tested in each experiment and control responses were compared with the responses obtained without the inhibitor within each ring. Since two consecutive concentration-response curves to NCA were generated for each aortic ring, the appropriate time-control experiment was performed (i.e. two consecutive concentration-response curves to NCA in the absence of the inhibitor). In one experiment, different inhibitors were added together to check their possible additive effect in the aortic rings.

The metal chelator diethylene triamine pentaacetic acid (DTPA) was always added to the buffer solution to limit the conversion of HNO to NO.

2.6 Mouse model of atherosclerosis

To investigate the role of the endothelium in the effect of NCA, two models of damaged endothelium were used. In the first model, endothelium was removed mechanically by inserting a stainless steel wire and gently rubbing the luminal side of the vessel [86]. In the second model, $ApoE^{-/-}$ mice were used [87]. The $ApoE^{-/-}$ mice were characterized by elevated plasma cholesterol and were provided by Prof. Dr. rer. nat. Dipl.-Biochem. Jörg Heeren, Department of Biochemistry, UKE. Verification of the endothelial damage *ex vivo* was confirmed in both models by failure of the vessel to relax in the presence of acetylcholine (ACh).

NCA was dissolved in dimethyl sulfoxide (DMSO) and stock solutions were kept frozen until use and protected from light. The structure and purity of NCA were always checked after its synthesis by King Laboratories (Department of Chemistry, Wake Forest University, Winston-Salem, North Carolina).

2.7 Statistical analysis

Results are presented as mean ± standard error of the mean (SEM), with *n* indicating the number of animals in each experiment. A statistical comparison of urinary levels of F_2-isoprostanes 8-iso-PGF2α, levels of F_2-isoprostane iPF2α-VI in the blood and systolic blood pressure was carried out using Student's t-test. The effects of NCA were analysed statistically by a repeated-measure analysis of variance (ANOVA) followed by the Bonferroni's post-test. A probability of less than 0.05 was considered to be significant.
The analysis of the data and plotting of the figures were performed using Graphpad Prism 4.0 software.

2.8 Animals

All animal care and experiments in this thesis were undertaken in accordance with German and European legislation regarding the use of animals for experimental protocols and all efforts were made to minimize animal suffering and to reduce the number of animals used.

2.9 Buffer recipes

Phosphate buffer

Dipotassium phosphate (K_2HPO_4)	13.3 g
Potassium dihydrogen phosphate (KH_2PO_4)	32.22 g
Sodium azide (NaN_3)	0.5 g
Sodium chloride (NaCl)	29.2 g
Ultrapure water at pH 7.4	q.s. 1000 mL

Extraction buffer

According to manufacturer's instructions

Modified Krebs solution

Sodium chloride (NaCl)	11.6 g
Potassium chloride (KCl)	0.7 g
Calcium chloride ($CaCl_2$)	0.7 g
Magnesium sulfate ($MgSO_4$)	0.6 g
Potassium dihydrogen phosphate (KH_2PO_4)	4.2 g
Sodium bicarbonate ($NaHCO_3$)	0.3 g
Glucose ($C_6H_{12}O_6$)	4.0 g
Ultrapure water at pH 7.4	q.s. 2000 mL

2.10 Chemicals

1H-[1,2,4]oxadizolo[4,3-a]quinoxalin-1-one (ODQ)	Sigma GmbH, Steinheim, Germany
1-Nitrosocyclohexyl acetate (NCA)	Wake Forest University, Alabama, USA
2,3,4,5,6-pentafluorobenzyl bromide (PFB)	Merck KgaA, Darmstadt, Germany
16,17,18,19-[$_2H^4$]-iPF$_{2\alpha}$-III	Cayman Chemical, Tallinn, Estonia
4-aminopyridine (4-AP)	Sigma GmbH, Steinheim, Germany
Acetone ($(CH_3)_2CO$)	Cayman Chemical, Michigan, USA
Acetonitrile (CH_3CN)	Sigma GmbH, Steinheim, Germany
Acetylcholine (ACh)	Sigma GmbH, Steinheim, Germany
Angeli's Salt ($Na_2N_2O_3$)	Cayman Chemical, Michigan, USA
Calcitonin gene-related peptide receptor fragment 8-37 (CGRP $_{8-37}$)	Sigma GmbH, Steinheim, Germany
Calcium chloride ($CaCl_2$)	Merck KgaA, Darmstadt, Germany
Diethylenetriamine pentaacetic acid (DTPA)	Merck KgaA, Darmstadt, Germany
Dimethyl sulfoxide (DMSO)	Merck KgaA, Darmstadt, Germany
Dipotassium phosphate (K_2HPO_4)	Merck KgaA, Darmstadt, Germany
Ellman's reagent (5,5'-dithiobis-(2-nitrobenzoic acid)	Cayman Chemical, Michigan, USA
Ethanol (C_2H_5OH)	Merck KgaA, Darmstadt, Germany
Glibenclamide	Sigma GmbH, Steinheim, Germany
Glucose ($C_6H_{12}O_6$)	Merck KgaA, Darmstadt, Germany
Heparin	Ratiopharm GmbH, Ulm, Germany
Hydrogene chloride (HCl) 30% (v/v)	Merck KgaA, Darmstadt, Germany
Iberiotoxin	Sigma GmbH, Steinheim, Germany
Isoprenaline ($C_{11}H_{17}NO$)	Sigma GmbH, Steinheim, Germany
Magnesium sulfate ($MgSO_4$)	Merck KgaA, Darmstadt, Germany
Methanol (CH_4O)	Merck KgaA, Darmstadt, Germany
Methylene chloride (CH_2Cl_2)	Merck KgaA, Darmstadt, Germany
N,*N*-Diisopropylethylamine, or Hünig's base ($C_8H_{19}N$)	Merck KgaA, Darmstadt, Germany
N,O-bis(trimethylsilyl) trifluoroacetamide (BSTFA)	Merck KgaA, Darmstadt, Germany
Potassium chloride (KCl)	Merck KgaA, Darmstadt, Germany
Potassium dihydrogen phosphate (KH_2PO_4)	Merck KgaA, Darmstadt, Germany
Prostaglandin $F_{2\alpha}$ ($PGF_{2\alpha}$)	Sigma GmbH, Steinheim, Germany
Reduced glutathione (GSH)	Sigma GmbH, Steinheim, Germany
Sodium azide (NaN_3)	Merck KgaA, Darmstadt, Germany

Sodium bicarbonate ($NaHCO_3$)	Merck KgaA, Darmstadt, Germany
Sodium chloride (NaCl)	Merck KgaA, Darmstadt, Germany
Monosodium citrate ($NaH_2C_6H_5O_7$)	Cayman Chemical, Michigan, USA
Tetraethylammonium chloride (TEA)	Sigma GmbH, Steinheim, Germany
Tetrahydro-2-furanyl-9H-purin-6-amine (SQ_{22536})	Sigma GmbH, Steinheim, Germany

2.11 Consumables

1,5- and 2-mL Eppis	Eppendorf AG, Hamburg, Germany
10-, 100- and 1000 µL pipette tips	Sarstedt AG Co, Nümbrecht, Germany
10-, 100-, and 1000 µL pipettes	Eppendorf AG, Hamburg, Germany
15 mL Falcon tubes	Sarstedt AG Co, Nümbrecht, Germany
25 mL serological pipettes	Sarstedt AG Co, Nümbrecht, Germany
5000 µL pipette tips	Eppendorf AG, Hamburg, Germany
Centrifugation tubes 15 mL	Sarstedt AG Co, Nümbrecht, Germany
Culture dishes 100 mm suregrip	Sarstedt AG Co, Nümbrecht, Germany
Glass envelopes	Schott AG, Mainz, Germany
Latex gloves	Kimberly-Clark, Zaventem, Belgium

2.12 Equipment

-80 °C Freezer	Kryotec, Hamburg, Germany
-20 °C Freezer	Liebherr, Rostock, Germany
4 – 8 °C Fridge	Liebherr, Rostock, Germany
96-well plate reader Sunrise	Tecan, Crailsheim, Germany
Accu jet pipetting aid	Eppendorf AG, Hamburg, Germany
Analytical balance	Sartorius AG, Göttingen, Germany
Arc lamp	Cairn Research, Kent, United Kingdom
Balance	Sartorius AG, Göttingen, Germany
Benchtop centrifuge Rotina 35 R	Hettich, Tuttlingen, Germany
Chemical balance	Sartorius AG, Göttingen, Germany
Fine dosage syringe 1 mL Omnifix F	B. Braun Melsungen AG, Melsungen, Germany
Force transducer Model TM50	Ingenieurbüro Jäckel, Hanau, Germany
GC-MS	Varian, Walnut Creek, USA
Hood with laminar vertical airflow	Heraeus, Hanau, Switzerland
Ice machine Scotsman AF10	Scotsman Ice Systems, Boksburg, USA

Magnetic stirrer	Heidolph Instruments GmbH & Co. KG, Schwabach, Germany
Metal hooks	Self-made by Center for Molecular Neurobiology Hamburg, Germany
Micro centrifuge 5415 R	Eppendorf AG, Hamburg, Germany
Orbital Shaker Heidoplh Titramax 101	Heidolph Instruments GmbH & Co. KG, Schwabach, Germany
Organ Chamber	Glasbläserei Brunswieg, Hamburg, Germany
pH-meter, digital	Knick, Berlin, Germany
Scalpel	Bayha GmbH, Tutlingen, Germany
Stereomicroscope	Carl Zeiss, Jena, Germany
Surgical forceps	Fine Science Tools GmbH, Heidelberg, Germany
Surgical scissors	Fine Science Tools GmbH, Heidelberg, Germany
Tail-cuff plethysmograph TSE 209000	TSE Systems, Bad Homburg, Germany
Ultra-Pure Water System	Millipore, Schwalbach, Germany
Vortexer Reax top	Heidolph Instruments GmbH & Co. KG, Schwabach, Germany
Water quench	Lauda Dr. R. Wobser GmbH, Lauda-Königshofen, Germany

2.13 Software

BeMon 2.61	Ingenieurbüro Jäckel, Hanau, Germany
BeMon Auswertung 2.61	Ingenieurbüro Jäckel, Hanau, Germany
ChemStation	Varian, Walnut Creek, USA
Endnote X3	Thomson Reuters, New York, USA
GIMP 2.6.6	GNOME Foundation, Groton, USA
Magellan Data Analysis Software	Tecan, Crailsheim, Germany
Office Excel 2007	Microsoft Corporation , Redmond, USA
Office Word 2011	Microsoft Corporation , Redmond, USA
Prism 4.0	GraphPad Software Incorporate, La Jolla, USA
Windows XP Professional	Microsoft Corporation , Redmond, USA

3 Results

3.1 Nitroxyl exacerbates oxidative stress *in vivo* after MCAO induction

Oxidative stress plays a central role in neuronal death in response to cerebral ischemia. Because HNO has been shown *in vitro* to mediate neuroprotection in part by scavenging oxidative stress, we thought to investigate the role of HNO in an *in vivo* mouse model of cerebral ischemia. *In vivo*, oxidative stress can be accurately measured by quantifying urinary excretion or plasma levels of F2-isoprostanes. Therefore, we measured F2-isoprostane 8-iso-PGF2a excretion in urine and F_2-isoprostane iPF2a-VI in blood in healthy mice and in mice subjected to MCAO. F2-isoprostane 8-iso-PGF2a excretion in urine, collected over a 6 h-period 1 day after MCAO induction was significantly elevated in mice injected with AS immediately prior to MCAO, compared to control mice (28.9 ± 2.7 ng/mg creatinine vs. 8.1 ± 5.3 ng/g creatinine; $p < 0.05$; Figure 1, left panel). In blood collected 2 days after MCAO, the F_2-isoprostane iPF2a-VI concentrations in mice treated with AS displayed a trend towards higher levels compared with control mice, but this difference was not statistically significant (Figure 1, right panel, control 957 ± 309 pg/mL; AS 1369 ± 473 pg/mL; $p = 0.34$).

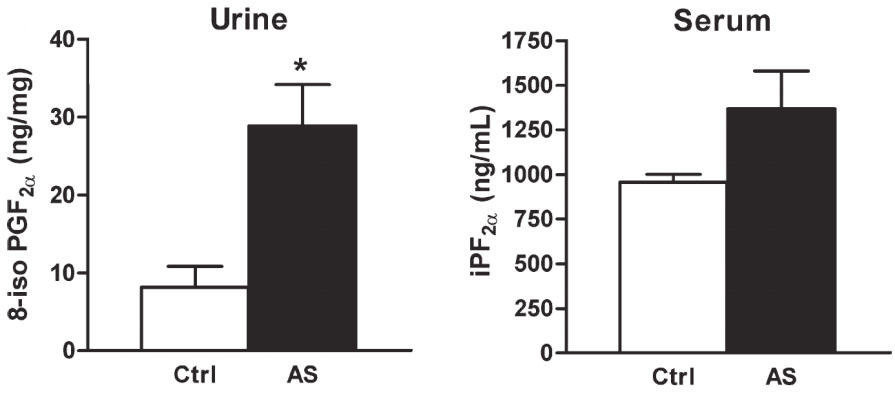

Figure 1: Oxidative stress levels in mice subjected to MCAO after AS or vehicle injection. Increased levels of urinary F_2-isoprostanes 8-iso-PGF2α (left panel) and blood F_2-isoprostane iPF2α-VI (right panel) in mice injected with AS. Results are expressed as mean ± SEM, n=4-9. **P*<0.05 vs. control.

3.2 Nitroxyl decreases systolic blood pressure *in vivo*

Because of the known vasorelaxant properties of AS [88], systolic blood pressure was non-invasively measured immediately and 30 min after i.p. injection of either AS (40 µmol/kg) or vehicle (10 mM NaOH). Blood pressure did not differ significantly immediately after AS injection (control 85 ± 14 mmHg; AS 76 ± 16 mmHg; p = 0.24; Figure 2, left panel). However, after 30 min we observed a decrease of approximately 30 mmHg (Figure 2, right panel, control 88 ± 22 mmHg; AS 57 ± 6 mmHg; p < 0.01). These results indicate a decreased blood perfusion associated with AS treatment, as expected.

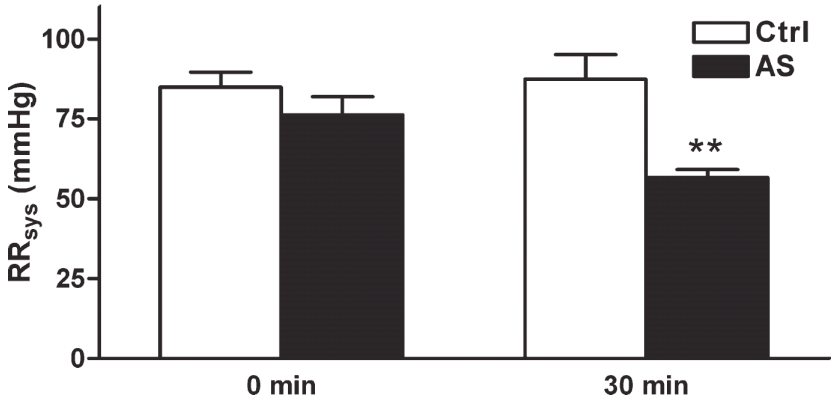

Figure 2: Systolic blood pressure levels in mice subjected to MCAO after AS or vehicle injection. Decreased systolic blood pressure after 30 min in mice injected with AS. Results are expressed as mean ± SEM, n=6. ***P*<0.01 vs. control.

3.3 Nitroxyl induces vasorelaxation in large arteries

Aortic rings isolated from WT mice were exposed to increasing concentrations of NCA (80 pM to 80 µM). NCA caused a concentration-dependent vasorelaxation in these vessels with an EC_{50} of 4.4 µM (n= 4-6, Figure 3A). The dependence of NCA-induced vasorelaxation on HNO was supported by the lack of effect observed with a structurally similar t-butyl ester of NCA, which does not hydrolyze to HNO, and DMSO, the vehicle for NCA (data not shown). In previous work, it has been suggested that HNO can be oxidized to NO via CuZn-SOD [83]. Therefore, to distinguish the effects of HNO from those of NO, we used glutathione (GSH) as thiol agent, because thiols act as a potent scavenger of HNO while having little effect on NO [15, 67]. Sodium nitroprusside (SNP) was used as an NO donor and GSH effect on SNP was compared to that of NCA. Addition of GSH (1 mM) to the extracellular medium resulted in ≈ 50% decrease in NCA (80 µM)-induced relaxation (n= 4-6, Figure 3A), while it had no effect on SNP-stimulated aortic rings (n= 4-6, Figure 3B). GSH itself caused no relaxation (data not shown). These results suggest that HNO is not converted to NO and that the effector species that induces vasorelaxation is HNO, rather than NO.

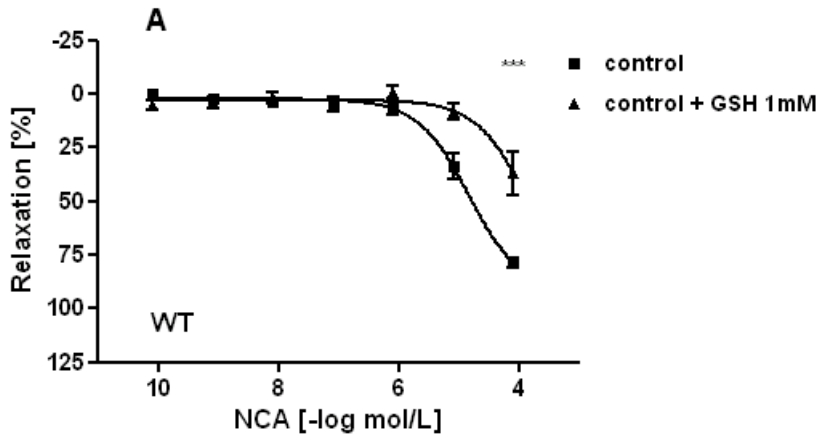

Figure 3A: Concentration-dependent effects of NCA in the absence or presence of GSH in wild-type mice aortic rings. GSH reduced the NCA-mediated vasorelaxation. The rings were pre-contracted with $PGF_{2\alpha}$ (5 µM). The relaxation effects were expressed as mean percentage ± SEM of decrement to the submaximal tension caused by $PGF_{2\alpha}$, n=4. ****P*< 0.001 vs. control.

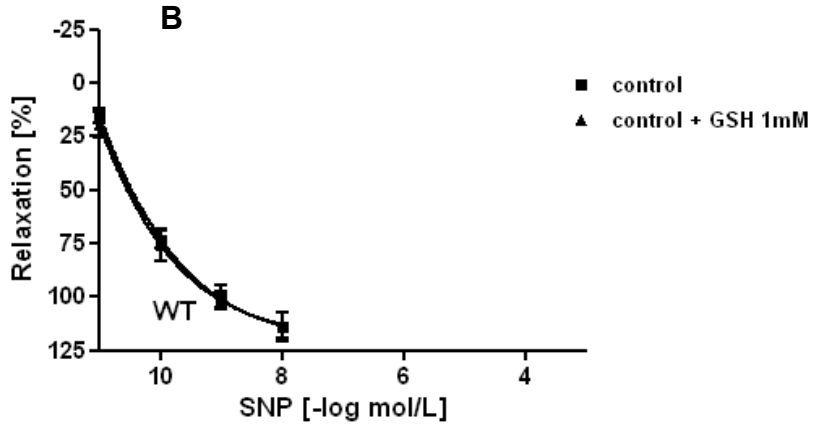

Figure 3B: Concentration-dependent effects of SNP in the absence or presence of GSH in wild-type mice aortic rings. GSH did not modify SNP-mediated vasorelaxation. The rings were pre-contracted with $PGF_{2\alpha}$ (5 µM). The relaxation effects were expressed as mean percentage ± SEM of decrement to the submaximal tension caused by $PGF_{2\alpha}$, n=4. **P*< 0.05 vs. control.

3.4 Signal transduction pathways in nitroxyl-mediated vasorelaxation

The mechanism of vasorelaxation induced by HNO released during the decomposition of NCA was deduced using a panel of pharmacologic inhibitors on aortic rings isolated from WT mice.

Role of sGC pathway in the vascular effects of nitroxyl

Nitric oxide (NO) activates the cytosolic enzyme sGC which catalyses the conversion of GTP to cGMP to induce vasorelaxation [89]. Therefore, the selective sGC inhibitor 1H-[1,2,4]oxadizolo[4,3-a]quinoxalin-1-one (ODQ, 5 µM) [72] was used to investigate the possible involvement of sGC in NCA effect. ODQ shifted the concentration-response curve of NCA to the right by ~1/2 an order of magnitude thereby reducing vasodilation effects (n= 6, Figure 4A) which is consistent with prior findings [91, 68, 93]. Since a previous study in aortae isolated from mice indicated that ODQ causes a concentration-dependent inhibition of HNO-mediated vasorelaxation [91], we tested a higher concentration of ODQ (10 µM) in this setting. ODQ failed to abolish NCA-induced vasorelaxation (data not shown). Therefore, we examined cGMP-independent mechanisms to investigate NCA-induced vasorelaxation.

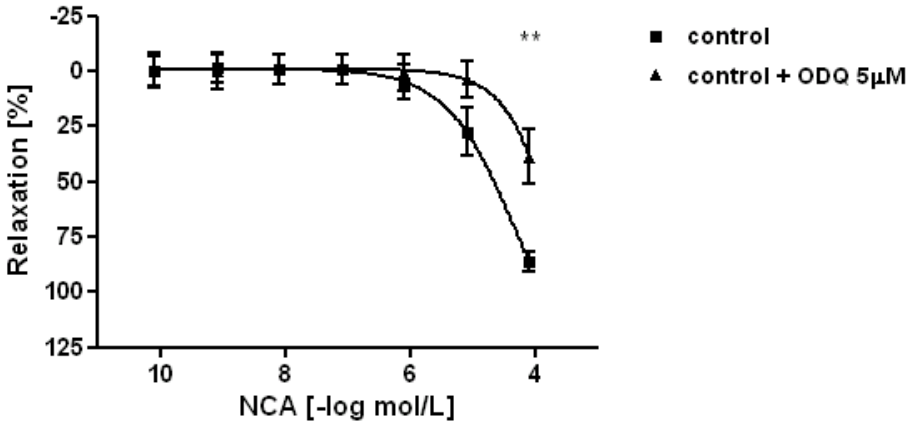

Figure 4A: Involvement of sGC in the vascular effects of NCA. Concentration-dependent effects of NCA in presence of ODQ, a sGC inhibitor. ODQ decreased NCA-mediated vasorelaxation. The relaxation effects were expressed as mean percentage ± SEM of decrement to the submaximal tension caused by $PGF_{2\alpha}$, n=4 ** $P< 0.01$ vs. control.

Role of AC pathway in the vascular effects of nitroxyl

β_1-adrenergic stimulation leads to the activation of adenylyl cyclase (AC) resulting in an increase in intracellular cyclic adenosine monophosphate (cAMP) levels and subsequently in the activation of Protein Kinase A leading vasorelaxation [93]. To investigate whether HNO effects are in part mediated by AC stimulation we used tetrahydro-2-furanyl-9H-purin-6-amine (SQ_{22536}, 100 µM [94]), a selective blocker of AC [95]. As control, we administered the β-adrenergic agonist isoprenaline. While SQ_{22536} completely blocked aortic ring relaxation induced by activation of AC via isoprenaline (data not shown), it had no influence on the vasorelaxation induced by NCA (n= 6, Figure 4B), suggesting that AC is not a target of HNO in the vasculature.

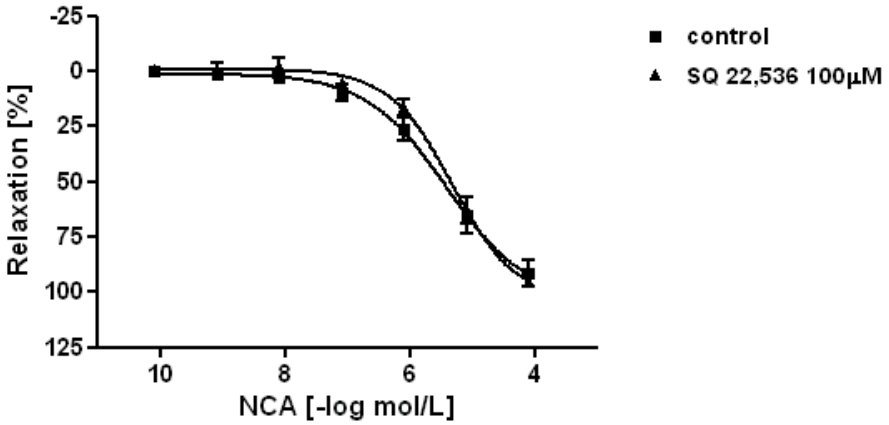

Figure 4B: Involvement of AC in the vascular effects of NCA. Concentration-dependent effects of NCA in presence of $SQ_{22,536}$, an AC inhibitor. $SQ_{22,536}$ did not modify NCA-mediated vasorelaxation. The rings were precontracted with $PGF_{2\alpha}$ (5 µM). The relaxation effects were expressed as mean percentage ± SEM of decrement to the submaximal tension caused by $PGF_{2\alpha}$, n=4-6. *P*> 0.05 vs. control.

Role of K^+ channels in the vascular effects of nitroxyl

Several potassium (K^+) channels play a major role in the regulation of vasculature tone [96]. To investigate whether these channels were involved in the action of NCA, we added to the organ bath the unselective K^+ channel blocker tetraethylammonium (TEA, 1 mM) [97]. After 30 min we observed an increase in the resting tension. The increase is a reproducibly manifest with a constant oscillation in the shape of a sine wave (~0.002 Hz.) This oscillation persisted until the end of the experimental setting. The effect of NCA was significantly reduced at NCA 80 µM in the TEA treated group versus control (n=4, Figure 5A, Control: 95.06 ± 3.787 SEM vs. NCA: 59.02 ±6.55 SEM), suggesting an involvement of K^+ channels in the action of HNO.

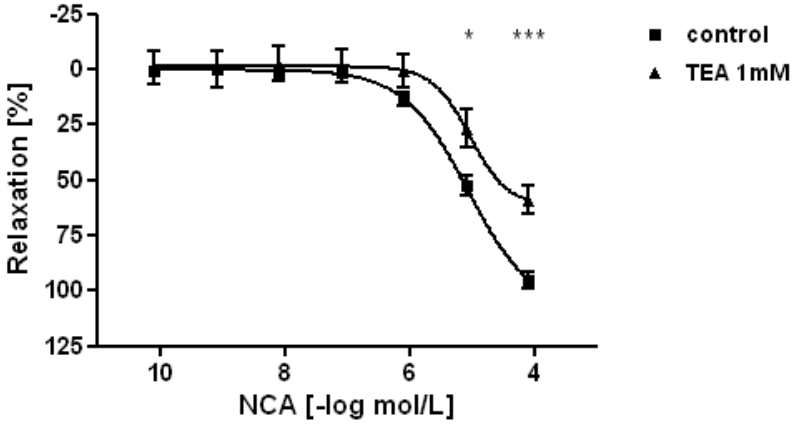

Figure 5A: Involvement of K^+ channels in the vascular effects of NCA. Concentration-dependent effects of NCA in presence of TEA, a non-selective K^+ channel blocker. TEA decreased NCA-

mediated vasorelaxation. The rings were precontracted with $PGF_{2\alpha}$ (5 µM). The relaxation effects were expressed as mean percentage ± SEM of decrement to the submaximal tension caused by $PGF_{2\alpha}$, n=4. * *P*< 0.05 vs. control. *** *P*< 0.001 vs. control.

Role of ATP-sensitive K^+ channels in the veascular effects of nitroxyl

The involvement of thiol-dependent redox mechanisms in ATP-sensitive K^+ channels (K_{ATP}) has been demonstrated in skeletal musculature [98]. Nevertheless, it is widely accepted that K_{ATP} are involved in the regulation of vascular tone as shown in previous work [99]. The aim of the present experiment was to investigate whether the activation of K_{ATP} can explain in part the vasorelaxation effect of HNO. For this reason, we used glibenclamide (1 µM), a well-known blocker of K_{ATP} [100]. The vasorelaxation effect of NCA was not affected by the presence of glibenclamide (n= 6, Figure 5B), suggesting no involvement of K_{ATP} in the action of NCA.

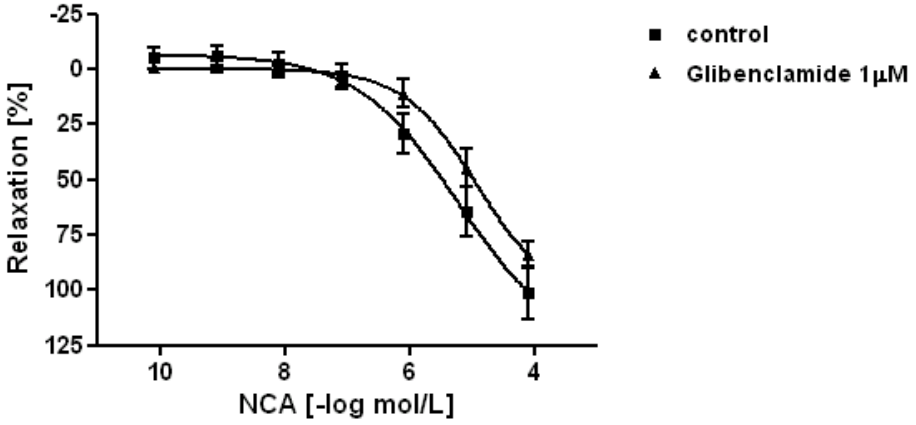

Figure 5B: Involvement of K_{ATP} channels in the vascular effects of NCA. Concentration-dependent effects of NCA in presence of glibenclamide, a K_{ATP} channels blocker. Glibenclamide did not modify NCA-mediated vasorelaxation. The rings were pre-contracted with $PGF_{2\alpha}$ (5 µM). The relaxation effects were expressed as mean percentage ± SEM of decrement to the submaximal tension caused by $PGF_{2\alpha}$, n=6. *P*> 0.05 vs. control.

Role of high-conductance Ca^{2+}-activated K^+ channels in the vascular effects of nitroxyl

Previous work has shown a critical role of redox modification of cysteine residues in the activity of high-conductance Ca^{2+}-activated K^+ channels (maxi-K) [101]. To investigate whether HNO mediates a redox modification of maxi-K channel, we used iberiotoxin (200 nM), a verum from the Indian red scorpion Buthus tamulus, for the selective inhibition of maxi-K channels [102]. As shown in Figure 5C, we observed similar effect of HNO in presence or absence of iberiotoxin, suggesting that maxi-K channels were not involved in the action of HNO.

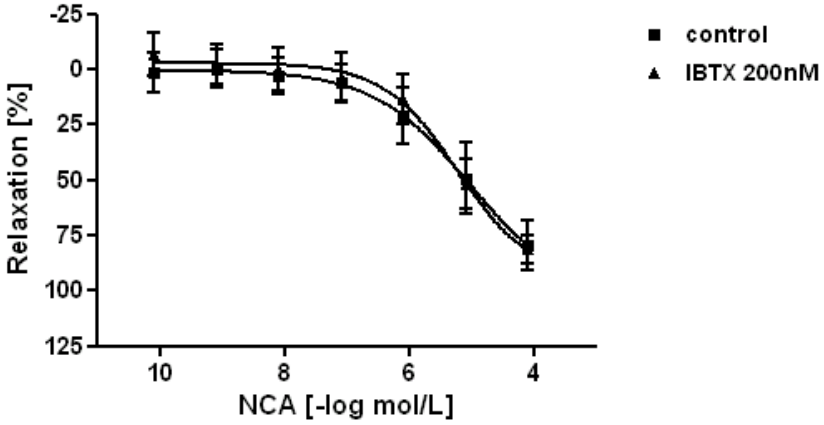

Figure 5C: Involvement of maxi-K channels in the vascular effects of NCA. Concentration-dependent effects of NCA in presence of iberiotoxin, a maxi-K channels blocker. Iberiotoxin did not modify NCA-mediated vasorelaxation. The rings were precontracted with $PGF_{2\alpha}$ (5 µM). The relaxation effects were expressed as mean percentage ± SEM of decrement to the submaximal tension caused by $PGF_{2\alpha}$, n=6. *P*> 0.05 vs. control.

Role of voltage-dependent K^+ channels in the vascular effects of nitroxyl

A thiol-based redox regulation of voltage-dependent K^+ channels (K_v) has been observed in previous work [103]. To examine a redox effect of HNO in the regulation of K_v, we used 4-aminopyridine (4-AP; 10 µM [104]) as specific blocker of K_v channels. We observed a stable increase in the resting tension, indicating that 4-AP was blocking K_v. Figure 5D shows a significant shift to the right of the concentration-response curve of NCA, indicating an involvement of these channels in HNO-induced vasorelaxation.

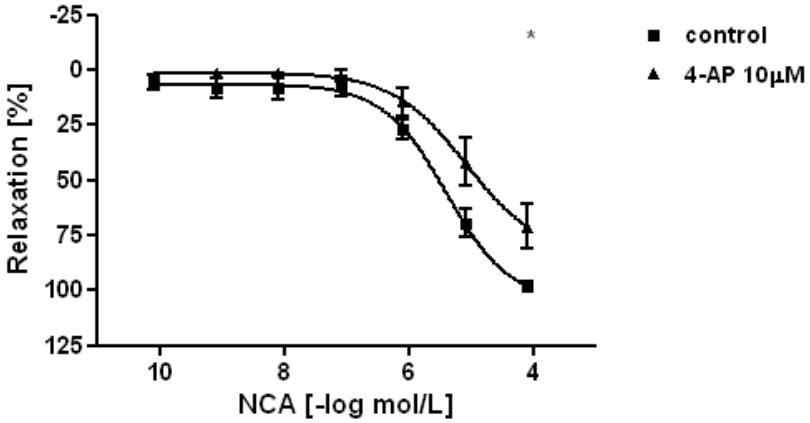

Figure 5D: Involvement of K_v channels in the vascular effects of NCA. Concentration-dependent effects of NCA in presence of 4-AP, a K_v channels blocker. 4-AP decreased NCA-mediated vasorelaxation. The rings were precontracted with $PGF_{2\alpha}$ (5 µM). The relaxation effects were

expressed as mean percentage ± SEM of decrement to the submaximal tension caused by $PGF_{2\alpha}$, n=6. * *P*< 0.05 vs. control.

Role of CGRP receptors in the effect of nitroxyl

Calcitonin gene-related peptide is considered to be one of the most potent vasodilators in biological systems [105]. In addition, it has been suggested that intravenous AS administration exerts positive cardiac inotropy via the stimulation of CGRP receptors *in vivo* [75]. Moreover, elevated plasma levels of calcitonin gene-related peptide have been observed after intravenous administration of AS in a model of cardiac failure induced by chronic tachycardia pacing *in vivo* [88]. To investigate whether HNO is able to interact with CGRP receptors *in vitro,* the calcitonin gene-related peptide receptor antagonist fragment 8-37 ($CGRP_{8-37}$, 1 µM) was added 30 min prior to NCA administration. Inhibition of CGRP receptors *in vitro* reduced the effect of NCA at 8 µM in the $CGRP_{8-37}$-treated group vs. control (n=4, Figure 6, NCA: 47.66 ± 14.27 SEM vs. control: 90.97 ± 7.20 SEM), suggesting an involvement of CGRP receptors in the mode of action of HNO.

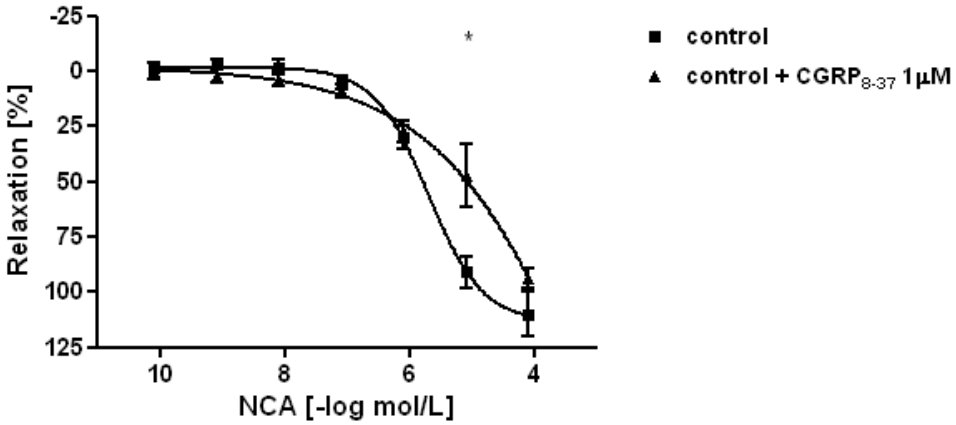

Figure 6: Involvement of CGRP receptors in the vascular effects of NCA. Concentration-dependent effects of NCA in presence of $CGRP_{8-37}$, a CGRP receptor antagonist. $CGRP_{8-37}$ decreased NCA-mediated vasorelaxation. The relaxation effects were expressed as mean percentage ± SEM of decrement to the submaximal tension caused by $PGF_{2\alpha}$, n=4. * *P*< 0.05 vs. control.

Effect of blocking sGC, CGRP receptors and K^+_v channels

Because sGC, voltage-dependent K^+ channels and CGRP receptors were involved in the HNO-mediated vasorelaxation, we thought whether blocking these three targets could abolish HNO effect. Therefore, we added in the organ bath, at the same time and 30 min prior to NCA administration, ODQ (5 µM), 4-AP (10 µM) and $CGRP_{8-37}$ (200 nM). This resulted in an increase in resting tension and, as shown in Figure 7, a sub-maximal

abolishment of the vasodilation effect of NCA, indicating that more possible targets are involved in the mechanisms of HNO.

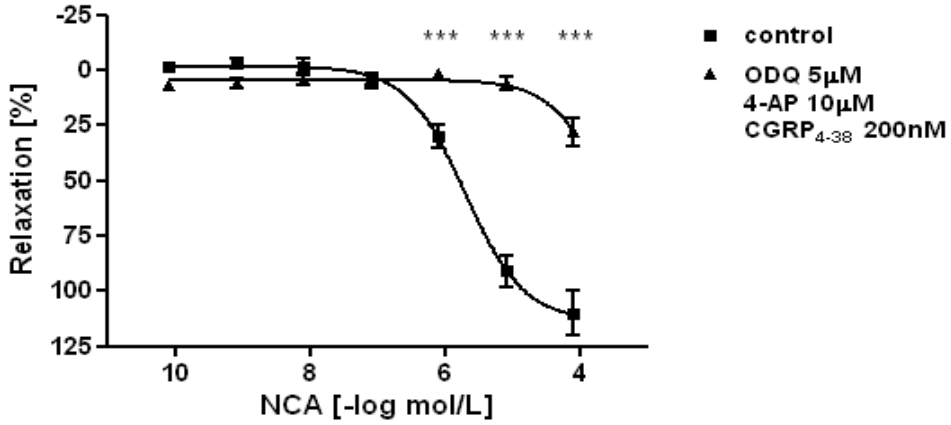

Figure 7: Inhibition of sGC, CGRP receptors and voltage dependent K^+ channels. Concentration-dependent effects of NCA in presence of ODQ (5 µM), 4-AP (10 µM) and $CGRP_{8-37}$ (200 nM). The three inhibitors reduced but not abolished NCA-mediated vasorelaxation. The relaxation effects were expressed as mean percentage ± SEM of decrement to the submaximal tension caused by $PGF_{2\alpha}$, n=4. *** $P< 0.001$ vs. control.

3.5 Nitroxyl induces vasorelaxation in ApoE$^{-/-}$ mice

Since the groundbreaking work of Furchgott [86] showing that endothelium is critical for the regulation of vasotone, it is widely accepted that NO formation in the endothelium leads to cGMP activation and subsequently to vasodilation [106]. To examine the effect of the endothelium in the HNO-mediated vasorelaxation, we compared the effect of NCA on aortic rings isolated from WT and ApoE$^{-/-}$ mice and in endothelial-denuded aortae. NCA (80 pM to 80 µM) caused a concentration-dependent vasorelaxation that was similar in all groups (EC50: 4.4 µM, n=6, Figure 8A), suggesting that HNO acts independently of the endothelium. We showed damage of the endothelium in ApoE$^{-/-}$ mice and in mechanically denuded aortic rings by measuring the dilatory response of isolated vessels in presence of acetylcholine (ACh). The effect of ACh was significantly reduced at NCA 80 µM in ApoE$^{-/-}$ vs. control (n=4, Figure 8B, ApoE$^{-/-}$: 43.35 ±9.30 SEM vs. control: 79.58 ±3.67 SEM). We observed similar results in endothelium-removed mice vs. control (n=4, Figure 8B, ApoE$^{-/-}$: 17.86 ±3.97 SEM vs. control: 79.58 ±3.67 SEM). These results suggest a significant damage of the

endothelium in ApoE$^{-/-}$ mice and in mechanically denuded aortic rings with subsequent endothelial dysfunction.

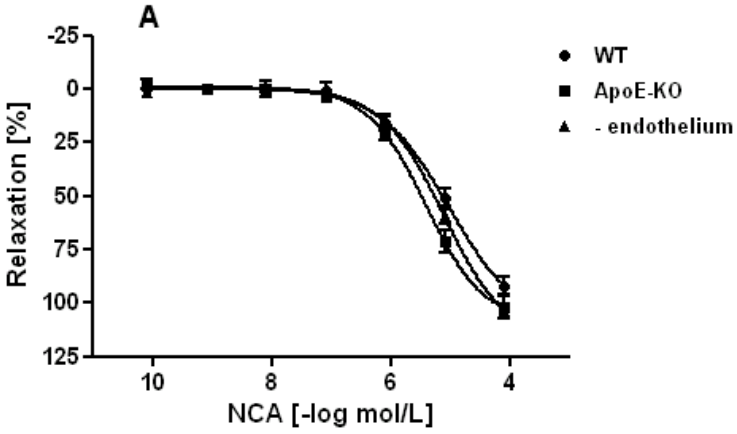

Figure 8A: Comparison of the vasodilator effects of NCA in healthy and damaged vasculature. NCA at increasing micromolar concentrations caused a potent and similar vasorelaxation of intact endothelium as well as damaged endothelium (ApoE$^{-/-}$ mice and mechanically endothelium-denuded aortae). The relaxation effects were expressed as mean percentage ± SEM of decrement to the submaximal tension caused by $PGF_{2\alpha}$, n=4-6.

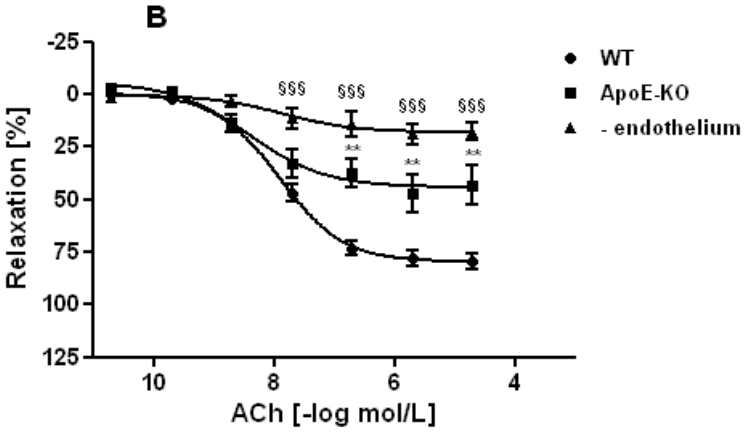

Figure 8B: Endothelial damage confirmed by failure of the vessel to relax, either partly or completely, in presence of acetylcholine (ACh). ACh effect was significantly reduced in ApoE$^{-/-}$ and in the endothelium-removed aortae. The relaxation effects were expressed as mean percentage ± SEM of decrement to the submaximal tension caused by $PGF_{2\alpha}$, n=4-6. §§§ P< 0.001 -endothelium vs. wild-type ** P< 0.01 ApoE-KO vs. wild- type.

4 Discussion

Previous *in vitro* reports have shown that HNO mediates neuroprotection by downregulation of excessive NMDA-evoked responses with subsequent decrease of excessive Ca^{2+} influx, therefore leading to decreased apoptotic signal cascades [60]. In addition, HNO has been shown to react directly with oxidants and to possess antioxidant properties [107]. Therefore, the ability of HNO to modulate NMDA receptor activity *in vitro*, in parallel with its ability to interact and scavenger oxidants, led us to hypothesize that HNO effects could apply as well to an *in vivo* model of cerebral ischemia. As *in vivo* mouse-stroke model, we used MCAO that is the most frequently used method to mimic permanent or transient focal cerebral ischemia in rodents [108], [109]. In collaboration with the Department of Neurology, UKE, we found that systemic administration of HNO has a detrimental effect in MCAO leading to an increased infarct size and an exacerbated persistent neurological deficit. In the first part of the present thesis, my main focus was to find possible explanations for the observed detrimental effects of HNO in this cerebral ischemia model. We found that increased isoprostanes levels in serum and urine, and reduced blood pressure *in vivo* were the cause for the observed HNO effects. Therefore, our current *in vivo* findings do not support the *in vitro* observations mentioned above. Oxidative stress is involved in ischemic neuronal death [110] and compromise of antioxidant mechanisms increase infarct size in animal models of ischemic stroke [111]. The nucleophilicity of HNO may accelerate the depletion of antioxidant reserves, in particular via oxidation of sacrificial thiol pools such as GSH [55]. In ischemic conditions where the oxygen levels are reduced, it is reasonable that oxidants formation should be increased. GSH is necessary to reduce oxidants formation even in healthy systems [112]. Therefore, depletion of GSH by HNO could lead to increased oxidants levels, augmented lipid peroxidation and thus elevation of isoprostanes levels. Furthermore, HNO may increase oxidative inflammatory interactions at the level of cerebral vessels, leading to an increased recruitment-extravasation of neutrophils and monocytes into ischemic brain parenchyma. An additional burden of leukocytic infiltrants would serve to worsen the severity of the injury and increase lesion size [113]. Feelisch and his group have already proposed a similar mechanism mediated by HNO during myocardial ischemia reperfusion [15]. Indeed, HNO was thought to exacerbate myocardial ischemia reperfusion injury through endothelial thiol oxidation and resultant increased neutrophil adhesion in afflicted zones [114]. However, further investigations are needed to determine whether these or other mechanisms may be contributing to injury in our experimental model.

Hypotension or drop of blood pressure in the arteries is aggravating clinical outcome of acute ischemic stroke [115]. Because HNO is known to be a potent vasorelaxant molecule [26], [76], [91], we sought to investigate whether these effects were preserved during vascular diseases

where it is observed damage in the endothelium. Figure 8A shows that HNO maintains its vasorelaxant effect in two different models of endothelium injury suggesting that HNO acts independently of the endothelium. Therefore, HNO-mediated hypotension in this model of cerebral ischemia-reperfusion injury may explain at least part of the deleterious neuronal effects of HNO. These results are in accordance with the view that HNO maintains its vasorelaxant effects during oxidative stress as shown by Leo were HNO effects were preserved in diabetes-induced oxidative stress [116]. In addition to the hypotensive effects, HNO may have local action on brain tissue. Indeed, HNO may enter into the brain by two possible mechanisms, disruption of the blood-brain barrier after cerebral ischemia, and significant increase in blood-brain barrier permeability after HNO administration [117], [118]. Further investigations are needed to verify this hypothesis.

The second part of my thesis was to elucidate the signaling pathway of HNO-mediated vasorelaxation. In large conduit arteries, mechanisms in addition to sGC activation are unknown [26]. The vasodilator effects of HNO on aorta were partially decreased by ODQ, suggesting contribution of sGC. This finding is consistent with prior reports [91], [68]. The underlying molecular mechanism is considered to be the activation of the ferrous but not ferric heme part of sGC [17]. Nevertheless, a study by Zeller indicates that HNO first requires oxidation to NO by SOD prior to appreciable activation of purified or endothelial sGC [119]. These findings suggest that HNO can activate sGC, yet intracellular oxidation of HNO to NO cannot be excluded. However, since ODQ failed to abolish HNO-induced vasorelaxation, the HNO effect may occur, at least in part, through a cGMP-independent mechanism and led us to examine several alternative pathways. CGRP, a potent relaxation-promoting peptide, has been implicated in HNO-mediated coronary vasodilation *ex vivo* and the CGRP-receptor antagonist suppressed the maximum vasodilator response to HNO by ~30% [76]. In our setting, $CGRP_{8-37}$ reduced the vasodilator response to HNO, suggesting that CGRP contribute partially to the vasorelaxation effect of HNO in isolated aortic rings. K^+ channels are a diverse and ubiquitous family of membrane proteins that play key roles in cellular signaling processes, such as smooth muscle contraction [120]. In vascular smooth muscle cells, opening K^+ channels promotes K^+ efflux, membrane repolarization, and closure of voltage-dependent Ca^{2+} channels, leading to relaxation. A wide variety of active intracellular messengers modify the activity of K^+ channels, including cGMP-dependent protein kinase [121]. Although at least four distinct types of K^+ channels are expressed in vascular smooth muscle cells, the vasodilator response to HNO was significantly inhibited by the non-selective K^+ channel blocker tetraethylammonium chloride and the selective K_v blocker 4-aminopyridine. By contrast, the K_{ATP} blocker glibenclamide or the maxi-K blocker iberiotoxin had no effect on NCA vasodilation. The exclusive involvement of K_v channels observed in the present study is consistent with similar findings in rat mesenteric arteries [92], but in contrast to that in the

coronary vasculature where an involvement of K_{ATP} has been demonstrated [68]. Whether HNO activation of K^+ channels is direct or cGMP-dependent remains to be elucidated; HNO-thiol interactions could enable the direct modulation of K_v channels independently of cGMP [68]. Overall, the involvement of sGC, CGRP and K_v channels in HNO-induced vasorelaxation is consistent with previous reports [76].

In summary, the present thesis has shown that HNO has a detrimental effect in an *in vivo* mouse-stroke model by increasing systemic oxidative stress and reducing blood pressure. The ability of HNO to reduce blood pressure was found to occur through a variety of pathways.

Limitations of the present study

It should be noted that despite many promising pre-clinical trials, no drugs are clinically used for neuroprotection in stroke [122]. This drawback leads to the investigation of neuroprotective agents [123]. A posteriori, the idea of improving the neurological outcome after MCAO by inactivating only one receptor, especially in complex medical conditions such as stroke, appears to be daring. Beyond this point, there are several methodical reasons that make it difficult to interpret our results. In our study there is no evidence that HNO released from Angeli´s salt was transported by the blood stream to the brain. In addition, there is no evidence for its passage through the blood-brain barrier. Temporary occlusion of the middle cerebral artery by insertion of a monofilament into the external carotid artery and advanced into the middle cerebral artery was initiated immediately after injection of AS to the mouse. The filament was removed after 1 h. Given that AS possess a half-life of 2.5 min and the intervention lasted for 1 h, it is unlikely that HNO would reach the neurons and enhance reperfusion damage. Thus, any consideration about the direct influence of HNO on neuronal damage is speculative. To provide evidence, AS should be isotopically labeled and its kinetics after intraperitoneal injection should be observed via positron emission tomography. However, the characterization of the pharmacokinetics of an agent with a half-life of 2.5 minutes will be very difficult. Nevertheless, assuming that AS/HNO does reach and pass through the blood-brain barrier, we were not able to show that the NMDA receptor is modulated *in vivo* by HNO. Studying NMDA receptor activity *in vivo* is very difficult and currently no methods are available to measure it.

Administration of AS was performed prior the induction of stroke. In clinical conditions, however, application of a neuroprotective agent for preventing cerebral ischemia reperfusion injury would be performed after stroke and before lysis. If we could have administered AS after middle brain artery occlusion, it could have been impossible for AS to reach the infarcted area, as mice have an insufficient circulus arteriosus cerebri willisii (the reason why

they are preferred for generating reproducible neuronal damage [124]). Unfortunately, so far all animal models of stroke lack portability to clinical situations. Thus, the implementation of new animal models of stroke could be a promising undertaking.

Regarding the elevated isoprostanes levels, it must be mentioned that although iPF_{2a} species are very specific markers for oxidative stress, they are unusable to determine its place of formation. The short half-life of AS and the intraperitoneal application suggests HNO release and possible harmful effects in intraperitoneal organs such as the bowels and liver. One way to prove it could be to monitor organ-specific biomarkers, like alanine aminotransferase or gamma glutamyltransferase, or to measure the effect of intraperitoneal application of AS on the iPF_{2a} levels without MCAO induction. In addition, the measurement of more neuron-specific markers of oxidative stress, like neurofurans may be an option [125].

Despite the various methodological problems occurred in the present thesis, we show that AS is harmful in ischemic stroke. However the exact mechanisms still remain unclear and demand further investigations.

Regarding the investigation of NCA effects and mechanism of action in the vasculature, I felt confident with the organ bath measurements, since this methodology is robust and well established. However, there are some points worth noting that make the interpretation of the results difficult.

After adding ODQ to the organ bath, I observed an increase in the resting tension of the aortic rings. It suggests that the inhibitor has reached its target molecule, in this case sGC. However, an elevated resting tension means that the vasodilator has to act against a greater force compared to the control group. Therefore, the observed influence on the mode of action of HNO could in part be explained simply by the increase in the resting tension. It explains why the starting conditions in the control and in the treated group might be different. An alternative setting could be to administer the inhibitor first, followed by a titration of PGF_{2a}. In this case, it would be possible to equalize the resting tension in both control and treated group. However, also in this case, the starting conditions will be different with respect to PGF_{2a} concentrations.

In contrast, inhibitors like iberiotoxin did not result in a change of the resting tension. It could be due to counter-regulation, such as the improved activation of sGC. Nevertheless, in this experimental setting there is no evidence for a blockage of Ca^{2+} channels by this inhibitor. Patch clamp techniques and x-ray crystal analysis may be useful tools to provide more evidence in the HNO-mediated activation of ion channels.

Concentration-response curves of NCA were obtained in the range from 80 pM to 80 µM. It is stated that NCA releases NO per se, but less than 1 % of total. Nonetheless, at 80 µM this equates to several hundred pM of NO. At this concentration, NO likely may have a vasorelaxant effect. Further experiments have been conducted by our workgroup in the

presence of an NO-scavenger like 2-4-carboxyphenyl-4,4,5,5-tetramethylmidazoline-1-oxyl-3-oxide (carboxy-PTIO). No reduction in NCA-mediated vasodilation could be shown. Another possibility is to perform fluorescence-activated cell sorting (FACS) analysis in smooth muscle cells incubated with NO-scavengers in direct comparison with direct NO-donors.

We were able to show an HNO-mediated effect via a CGRP pathway *in vitro* [126]. However, we have no evidence for the underlying molecular process of this observation. Several mechanisms are possible and require intensive investigations, such as HNO-mediated release of CGRP from intramuscular synaptic endings, the direct activation of CGRP receptors or the enhancement of the downstream cascade relating to CGRP receptors.

Another observation is that NCA-mediated vasorelaxation is reversible. Interestingly, until now there are no reports about mechanisms which retract the effects of HNO *in vivo* or *in vitro*.

5 Summary

Around 100 years after its discovery by the Italian chemist Angelo Angeli, nitroxyl (HNO), the one-electron reduced form of nitric oxide, is enjoying a renaissance. Several reports have shown numerous beneficial effects of HNO in the cardiovascular system, leading HNO releasing donor compounds to emerge as promising therapeutic reagents for treating cardiovascular-related diseases, with pre-clinical trials ongoing. In contrast, the role of HNO in the central nervous system is less well understood. In the present thesis, we have studied the effect of HNO using AS in a well-established model of cerebral ischemia, the middle cerebral artery occlusion, in mice. We demonstrate that HNO exacerbates the cerebral infarct size and the permanent neurological deficit in MCAO model. The increased injury was associated with a drop in systolic blood pressure and an increase in systemic oxidative stress. Importantly, the micromolar concentrations of HNO shown to be detrimental in the nervous system have been shown to be cardioprotective. Therefore, the presented data highlight the uniquely different functions of HNO in the cardiovascular and central nervous systems with respect to effects on ischemia-reperfusion injury.
Furthermore, we have shown that HNO released from NCA (the newest NCA donor compound) lowers blood pressure through a variety of pathways, and maintain its vasorelaxant effect in a diseased vascular system.

Rund 100 Jahre nach seiner Entdeckung durch den italienischen Chemiker Angelo Angeli erlebt Nitroxyl (HNO), die einfach reduzierte Form von Stickstoffmonoxid, eine Renaissance. Zahlreiche Arbeiten zeigten positive Effekte von HNO im kardiovaskulären System. Im Gegensatz dazu ist die Rolle von HNO im zentralen Nervensystem kaum verstanden. In der vorliegenden Arbeit wurden zunächst die Effekte von HNO beziehungsweise seines gängigen Donators AS in einem etablierten Schlaganfallmodell in der Maus untersucht. Wir konnten zeigen, dass die Größe des Schlaganfalls nach histologischen Kriterien zunahm und sich das klinisch neurologisch Outcome der Mäuse unter AS Applikation verschlechterte. Als ursächlich hierfür zeigte sich eine hypotensive Blutdrucksituation sowie eine Zunahme des oxidativen Stress. Die gewählte AS-Konzentration war vergleichbar mit derer, die in den Vorarbeiten einen kardioprotektiven Effekt gezeigt hatte.
Zusätzlich wurde in dieser Arbeit ein neuartiger HNO Donor, namentlich NCA bezüglich seiner Pharmakodynamik untersucht und es konnten verschiedene Wirkmechanismen aufgeklärt werden über die es zu einer Vasorelaxation, auch in pathologisch veränderten Gefäßen, kommt.

6 Abbreviations

° C	Degree Celsius
AC	Adenyl cyclase
ALDH-2	Aldehyddehydrogenase 2
ANOVA	Analysis of variance
ApoE	Apolipoprotein E
AS	Angeli's Salt
ATP	Adenosine triphosphate
Ca^{2+}	Calcium ion
cAMP	Cyclic adenosine monophosphate
cGMP	Cyclic guanosine monophosphate
CGRP	Calcitonin-related peptide
DNA	Deoxyribonucleic acid
EIA	Enzymeimmunoassay
ELISA	Enzyme-linked immunosorbent assay
eV	Electronvolt
FACS	Fluorescence-activated cell sorting
g	Gram
GAPDH	Glyceraldehyde-3-phosphate dehydrogenase
GCMS	Gas chromatography mass spectrometry
GTP	Guanosine-5'-triphosphate
h	Hour
H_2S	Hydrogen sulphide
$[Ca^{2+}]_i$	Intracellular calcium level
$iPF_{2\alpha}$	Isoprostane prostaglandine F2α
IU	International Unit
JNK	c-Jun N-terminal kinase
K^+	Potassium ion
K_{ATP}	ATP-sensitive potassium channel
KO	Knockout
kV	Kilovolt
K_v	Voltage-dependent potassium channel
LDL	Low density lipoprotein
m	Meter
M	Molar
maxi-K	High conductance Ca^{2+} activated K^+

MCAO	Middle brain artery occlusion
min	Minute
mL	Milliliter
mm	Millimeter
NCA	1-Nitrosocyclohexyl acetate.
ng	Nanogram
nm	Nanometer
NMDA	N-methyl-D-aspartate
NO	Nitric oxide
NOS	Nitric oxide synthase
pg	Picogram
pK_a	Equilibrium constant
q.s.	quantum satis (up to)
ROS	Reactive oxygen species
Ryr2	Ryanodine receptors
s	Second
SEM	Standard error of the mean
SERCA	Sarcoplasmic/endoplasmic reticulum calcium ATPase
sGC	Soluble guanylcyclase
SOD	Superoxide dismutase
SR	Sarcoplasmatic reticulum
$t_{1/2}$	Half-life
UKE	University Medical Center Hamburg-Eppendorf
vs.	Versus
µL	Microliter

7 Bibliography

1. Moncada S, Higgs EA. The discovery of nitric oxide and its role in vascular biology. *Br. J. Pharmacol.* 2006; 147 Suppl 1:S193–201.

2. Moncada S, Higgs EA. Endogenous nitric oxide: physiology, pathology and clinical relevance. *Eur. J. Clin. Invest.* 1991; 21:361–374.

3. Garthwaite J, Charles SL, Chess-Williams R. Endothelium-derived relaxing factor release on activation of NMDA receptors suggests role as intercellular messenger in the brain. *Nature*. 1988; 336:385–8.

4. Bolanos JP, Peuchen S, Heales SJ, Land JM, Clark JB. Nitric oxide-mediated inhibition of the mitochondrial respiratory chain in cultured astrocytes. *J Neurochem*. 1994; 63:910–6.

5. Hibbs JB Jr. Synthesis of nitric oxide from L-arginine: a recently discovered pathway induced by cytokines with antitumour and antimicrobial activity. *Res Immunol*. 1991; 142:565–9; discussion 596–8.

6. Kanner J, Harel S, Granit R. Nitric oxide as an antioxidant. *Arch Biochem Biophys*. 1991; 289:130–6.

7. Nguyen T, Brunson D, Crespi CL, Penman BW, Wishnok JS, Tannenbaum SR. DNA damage and mutation in human cells exposed to nitric oxide in vitro. *Proc Natl Acad Sci U S A*. 1992; 89:3030–4.

8. Jenkins DC, Charles IG, Thomsen LL, Moss DW, Holmes LS, Baylis SA, Rhodes P, Westmore K, Emson PC, Moncada S. Roles of nitric oxide in tumor growth. *Proc Natl Acad Sci U S A*. 1995; 92:4392–6.

9. Radi R, Beckman JS, Bush KM, Freeman BA. Peroxynitrite-induced membrane lipid peroxidation: the cytotoxic potential of superoxide and nitric oxide. *Arch Biochem Biophys*. 1991; 288:481–7.

10. Cleeter MW, Cooper JM, Darley-Usmar VM, Moncada S, Schapira AH. Reversible inhibition of cytochrome c oxidase, the terminal enzyme of the mitochondrial respiratory chain, by nitric oxide. Implications for neurodegenerative diseases. *FEBS Lett*. 1994; 345:50–4.

11. Caulfield JL, Wishnok JS, Tannenbaum SR. Nitric oxide-induced deamination of cytosine and guanine in deoxynucleosides and oligonucleotides. *J Biol Chem*. 1998; 273:12689–95.

12. Bonfoco E, Krainc D, Ankarcrona M, Nicotera P, Lipton SA. Apoptosis and necrosis: two distinct events induced, respectively, by mild and intense insults with N-methyl-D-aspartate or nitric oxide/superoxide in cortical cell cultures. *Proc Natl Acad Sci U S A*. 1995; 92:7162–6.

13. Shafirovich V, Lymar SV. Nitroxyl and its anion in aqueous solutions: spin states, protic equilibria, and reactivities toward oxygen and nitric oxide. *Proc Natl Acad Sci U S A*. 2002; 99:7340–5.

14. Shafirovich V, Lymar SV. Spin-forbidden deprotonation of aqueous nitroxyl (HNO). *J Am Chem Soc*. 2003; 125:6547–52.

15. Pino RZ, Feelisch M. Bioassay discrimination between nitric oxide (NO.) and nitroxyl (NO-) using L-cysteine. *Biochem. Biophys. Res. Commun.* 1994; 201:54–62.

16. Miranda KM, Nims RW, Thomas DD, Espey MG, Citrin D, Bartberger MD, Paolocci N, Fukuto JM, Feelisch M, Wink DA. Comparison of the reactivity of nitric oxide and nitroxyl with heme proteins. A chemical discussion of the differential biological effects of these redox related products of NOS. *J Inorg Biochem*. 2003; 93:52–60.

17. Miller TW, Cherney MM, Lee AJ, Francoleon NE, Farmer PJ, King SB, Hobbs AJ, Miranda KM, Burstyn JN, Fukuto JM. The effects of nitroxyl (HNO) on soluble guanylate cyclase activity: interactions at ferrous heme and cysteine thiols. *J Biol Chem*. 2009; 284:21788–96.

18. Wong PS, Hyun J, Fukuto JM, Shirota FN, DeMaster EG, Shoeman DW, Nagasawa HT. Reaction between S-nitrosothiols and thiols: generation of nitroxyl (HNO) and subsequent chemistry. *Biochemistry*. 1998; 37:5362–71.

19. Hoffman MD, Walsh GM, Rogalski JC, Kast J. Identification of nitroxyl-induced modifications in human platelet proteins using a novel mass spectrometric detection method. *Mol. Cell Proteomics*. 2009; 8:887–903.

20. Farmer PJ, Sulc F. Coordination chemistry of the HNO ligand with hemes and synthetic coordination complexes. *J Inorg Biochem*. 2005; 99:166–84.

21. Doyle MP, Mahapatro SN, Broene RD, Guy JK. Oxidation and reduction of hemoproteins by trioxodinitrate(II). The role of nitrosyl hydride and nitrite. *Journal of the American Chemical Society*. 1988; 110:593–599.

22. Doyle MP, Pickering RA, Da Conceição J. Structural effects in alkyl nitrite oxidation of human hemoglobin. *J. Biol. Chem.* 1984; 259:80–87.

23. Tocchetti CG, Wang W, Froehlich JP, Huke S, Aon MA, Wilson GM, Di Benedetto G, O'Rourke B, Gao WD, Wink DA, Toscano JP, Zaccolo M, Bers DM, Valdivia HH, Cheng H, Kass DA, Paolocci N. Nitroxyl improves cellular heart function by directly enhancing cardiac sarcoplasmic reticulum Ca2+ cycling. *Circ Res*. 2007; 100:96–104.

24. Bullen ML, Miller AA, Dharmarajah J, Drummond GR, Sobey CG, Kemp-Harper BK. Vasorelaxant and antiaggregatory actions of the nitroxyl donor isopropylamine NONOate are maintained in hypercholesterolemia. *Am J Physiol Heart Circ Physiol*. 2011; 301:H1405–14.

25. Choe C, Lewerenz J, Fischer G, Uliasz TF, Espey MG, Hummel FC, King SB, Schwedhelm E, Böger RH, Gerloff C, Hewett SJ, Magnus T, Donzelli S. Nitroxyl exacerbates ischemic cerebral injury and oxidative neurotoxicity. *J. Neurochem.* 2009; 110:1766–1773.

26. Fukuto JM, Chiang K, Hszieh R, Wong P, Chaudhuri G. The pharmacological activity of nitroxyl: a potent vasodilator with activity similar to nitric oxide and/or endothelium-derived relaxing factor. *J Pharmacol Exp Ther*. 1992; 263:546–51.

27. Adak S, Wang Q, Stuehr DJ. Arginine conversion to nitroxide by tetrahydrobiopterin-free neuronal nitric-oxide synthase. Implications for mechanism. *J Biol Chem*. 2000; 275:33554–61.

28. Hobbs AJ, Fukuto JM, Ignarro LJ. Formation of free nitric oxide from l-arginine by nitric oxide synthase: direct enhancement of generation by superoxide dismutase. *Proc Natl Acad Sci U S A*. 1994; 91:10992–6.

29. Saleem M, Ohshima H. Xanthine oxidase converts nitric oxide to nitroxyl that inactivates the enzyme. *Biochem. Biophys. Res. Commun.* 2004; 315:455–462.

30. Donzelli S, Espey MG, Flores-Santana W, Switzer CH, Yeh GC, Huang J, Stuehr DJ, King SB, Miranda KM, Wink DA. Generation of nitroxyl by heme protein-mediated peroxidation of hydroxylamine but not N-hydroxy-L-arginine. *Free Radic Biol Med*. 2008; 45:578–84.

31. Eberhardt M, Dux M, Namer B, Miljkovic J, Cordasic N, Will C, Kichko TI, De la Roche J, Fischer M, Suárez SA, Bikiel D, Dorsch K, Leffler A, Babes A, Lampert A, Lennerz JK, Jacobi J, Martí MA, Doctorovich F, Högestätt ED, Zygmunt PM, Ivanovic-Burmazovic I, Messlinger K, Reeh P, Filipovic MR. H2S and NO cooperatively regulate vascular tone by activating a neuroendocrine HNO-TRPA1-CGRP signalling pathway. *Nat Commun*. 2014; 5:4381.

32. Kemp-Harper BK. Nitroxyl (HNO): a novel redox signaling molecule. *Antioxid Redox Signal*. 2011; 14:1609–13.

33. Nakagawa H. Controlled release of HNO from chemical donors for biological applications. *J Inorg Biochem*. 2013; 118:187–90.

34. Hughes MN, Wimbledon PE. The chemistry of trioxodinitrates. Part 2. The effect of added nitrite on the stability of sodium trioxodinitrate in aqueous solution. *Journal of the Chemical Society, Dalton Transactions* [Internet]. 1977;Available from: http://dx.doi.org/10.1039/DT9770001650

35. Angeli A. Sopra il nitroso dell' isosafrolo. *Gazz- Chim. Ital.* 1896; 26:7–12.

36. Bonner FT, Ravid B. Thermal decomposition of oxyhyponitrite (sodium trioxodinitrate(II)) in aqueous solution. *Inorganic Chemistry*. 1975; 14:558–563.

37. Gladwin MT, Raat NJ, Shiva S, Dezfulian C, Hogg N, Kim-Shapiro DB, Patel RP. Nitrite as a vascular endocrine nitric oxide reservoir that contributes to hypoxic signaling, cytoprotection, and vasodilation. *Am J Physiol Heart Circ Physiol*. 2006; 291:H2026–35.

38. Sha X, Isbell TS, Patel RP, Day CS, King SB. Hydrolysis of acyloxy nitroso compounds yields nitroxyl (HNO). *J Am Chem Soc*. 2006; 128:9687–92.

39. Shoman ME, DuMond JF, Isbell TS, Crawford JH, Brandon A, Honovar J, Vitturi DA, White CR, Patel RP, King SB. Acyloxy nitroso compounds as nitroxyl (HNO) donors: kinetics, reactions with thiols, and vasodilation properties. *J Med Chem*. 2011; 54:1059–70.

40. Lopez AD, Mathers CD, Ezzati M, Jamison DT, Murray CJ. Global and regional burden of disease and risk factors, 2001: systematic analysis of population health data. *Lancet*. 2006; 367:1747–57.

41. Roger VL, Go AS, Lloyd-Jones DM, Adams RJ, Berry JD, Brown TM, Carnethon MR, Dai S, De Simone G, Ford ES, Fox CS, Fullerton HJ, Gillespie C, Greenlund KJ, Hailpern SM, Heit JA, Ho PM, Howard VJ, Kissela BM, Kittner SJ, Lackland DT, Lichtman JH, Lisabeth LD, Makuc DM, Marcus GM, Marelli A, Matchar DB, McDermott MM, Meigs JB, Moy CS, Mozaffarian D, Mussolino ME, Nichol G, Paynter NP, Rosamond WD, Sorlie PD, Stafford RS, Turan TN, Turner MB, Wong ND, Wylie-Rosett J. Heart disease and stroke statistics--2011 update: a report from the American Heart Association. *Circulation*. 2011; 123:e18–e209.

42. Kolominsky-Rabas PL, Heuschmann PU, Marschall D, Emmert M, Baltzer N, Neundorfer B, Schoffski O, Krobot KJ. Lifetime cost of ischemic stroke in Germany: results and national projections from a population-based stroke registry: the Erlangen Stroke Project. *Stroke*. 2006; 37:1179–83.

43. Caplan L, Chung C-S, Wityk R, Glass T, Tapia J, Pazdera L, Chang H-M, Dashe J, Chaves C, Vemmos K, Leary M, Dewitt L, Pessin M. New England medical center posterior circulation stroke registry: I. Methods, data base, distribution of brain lesions, stroke mechanisms, and outcomes. *J Clin Neurol*. 2005; 1:14–30.

44. Burmester T, Hankeln T. Neuroglobin: a respiratory protein of the nervous system. *News Physiol Sci*. 2004; 19:110–3.

45. Symon L, Branston NM, Strong AJ, Hope TD. The concepts of thresholds of ischaemia in relation to brain structure and function. *J Clin Pathol Suppl (R Coll Pathol)*. 1977; 11:149–54.

46. Hamann GF. [Acute cerebral infarct: physiopathology and modern therapeutic concepts]. *Radiologe*. 1997; 37:843–52.

47. Choi DW. Glutamate neurotoxicity and diseases of the nervous system. *Neuron*. 1988; 1:623–34.

48. Limbrick DD Jr, Churn SB, Sombati S, DeLorenzo RJ. Inability to restore resting intracellular calcium levels as an early indicator of delayed neuronal cell death. *Brain Res*. 1995; 690:145–56.

49. Bruno V, Copani A, Battaglia G, Dell'Albani P, Condorelli DF, Nicoletti F. Metabotropic glutamate receptors and neuronal degeneration in culture. *Adv Neurol*. 1996; 71:47–51, discussion 51–2.

50. Culmsee C, Krieglstein J. Ischaemic brain damage after stroke: new insights into efficient therapeutic strategies. International Symposium on Neurodegeneration and Neuroprotection. *EMBO Rep*. 2007; 8:129–33.

51. Astrup J, Symon L, Branston NM, Lassen NA. Cortical evoked potential and extracellular K+ and H+ at critical levels of brain ischemia. *Stroke*. 1977; 8:51–7.

52. Morrow JD, Hill KE, Burk RF, Nammour TM, Badr KF, Roberts LJ 2nd. A series of prostaglandin F2-like compounds are produced in vivo in humans by a non-cyclooxygenase, free radical-catalyzed mechanism. *Proc Natl Acad Sci U S A*. 1990; 87:9383–7.

53. Rokach J, Khanapure SP, Hwang SW, Adiyaman M, Lawson JA, FitzGerald GA. Nomenclature of isoprostanes: a proposal. *Prostaglandins*. 1997; 54:853–873.

54. Tsikas D, Schwedhelm E, Suchy MT, Niemann J, Gutzki FM, Erpenbeck VJ, Hohlfeld JM, Surdacki A, Frolich JC. Divergence in urinary 8-iso-PGF(2alpha) (iPF(2alpha)-III, 15-F(2t)-IsoP) levels from gas chromatography-tandem mass spectrometry quantification after thin-layer chromatography and immunoaffinity column chromatography reveals heterogeneity of 8-iso-PGF(2alpha). Possible methodological, mechanistic and clinical implications. *J Chromatogr B Analyt Technol Biomed Life Sci*. 2003; 794:237–55.

55. Donzelli S, Espey MG, Thomas DD, Mancardi D, Tocchetti CG, Ridnour LA, Paolocci N, King SB, Miranda KM, Lazzarino G, Fukuto JM, Wink DA. Discriminating formation of

HNO from other reactive nitrogen oxide species. *Free Radic Biol Med*. 2006; 40:1056–66.

56. Nagasawa HT, DeMaster EG, Redfern B, Shirota FN, Goon DJ. Evidence for nitroxyl in the catalase-mediated bioactivation of the alcohol deterrent agent cyanamide. *J Med Chem*. 1990; 33:3120–2.

57. Vaananen AJ, Kankuri E, Rauhala P. Nitric oxide-related species-induced protein oxidation: reversible, irreversible, and protective effects on enzyme function of papain. *Free Radic Biol Med*. 2005; 38:1102–11.

58. Kim WK, Choi YB, Rayudu PV, Das P, Asaad W, Arnelle DR, Stamler JS, Lipton SA. Attenuation of NMDA receptor activity and neurotoxicity by nitroxyl anion, NO. *Neuron*. 1999; 24:461–9.

59. Colton CA, Gbadegesin M, Wink DA, Miranda KM, Espey MG, Vicini S. Nitroxyl anion regulation of the NMDA receptor. *J Neurochem*. 2001; 78:1126–34.

60. Lipton SA, Choi YB, Pan ZH, Lei SZ, Chen HS, Sucher NJ, Loscalzo J, Singel DJ, Stamler JS. A redox-based mechanism for the neuroprotective and neurodestructive effects of nitric oxide and related nitroso-compounds. *Nature*. 1993; 364:626–632.

61. Cighetti G, Allevi P, Debiasi S, Paroni R. Inhibition of in vitro lipid peroxidation by stable steroidic nitroxyl radicals. *Chem Phys Lipids*. 1997; 88:97–106.

62. Libby P, Ridker PM, Hansson GK. Progress and challenges in translating the biology of atherosclerosis. *Nature*. 2011; 473:317–25.

63. Lewington S, Clarke R, Qizilbash N, Peto R, Collins R. Age-specific relevance of usual blood pressure to vascular mortality: a meta-analysis of individual data for one million adults in 61 prospective studies. *Lancet*. 2002; 360:1903–13.

64. Staessen JA, Fagard R, Thijs L, Celis H, Arabidze GG, Birkenhager WH, Bulpitt CJ, De Leeuw PW, Dollery CT, Fletcher AE, Forette F, Leonetti G, Nachev C, O'Brien ET, Rosenfeld J, Rodicio JL, Tuomilehto J, Zanchetti A. Randomised double-blind comparison of placebo and active treatment for older patients with isolated systolic hypertension. The Systolic Hypertension in Europe (Syst-Eur) Trial Investigators. *Lancet*. 1997; 350:757–64.

65. Collins R, Peto R, MacMahon S, Hebert P, Fiebach NH, Eberlein KA, Godwin J, Qizilbash N, Taylor JO, Hennekens CH. Blood pressure, stroke, and coronary heart disease. Part 2, Short-term reductions in blood pressure: overview of randomised drug trials in their epidemiological context. *Lancet*. 1990; 335:827–38.

66. Mancia G, Fagard R, Narkiewicz K, Redon J, Zanchetti A, Böhm M, Christiaens T, Cifkova R, De Backer G, Dominiczak A, Galderisi M, Grobbee DE, Jaarsma T, Kirchhof P, Kjeldsen SE, Laurent S, Manolis AJ, Nilsson PM, Ruilope LM, Schmieder RE, Sirnes PA, Sleight P, Viigimaa M, Waeber B, Zannad F. 2013 ESH/ESC Practice Guidelines for the Management of Arterial Hypertension. *Blood Press.* 2014; 23:3–16.

67. Ellis A, Li CG, Rand MJ. Differential actions of L-cysteine on responses to nitric oxide, nitroxyl anions and EDRF in the rat aorta. *Br J Pharmacol*. 2000; 129:315–22.

68. Irvine JC, Favaloro JL, Kemp-Harper BK. NO- activates soluble guanylate cyclase and Kv channels to vasodilate resistance arteries. *Hypertension*. 2003; 41:1301–7.

69. Dautov RF, Ngo DTM, Licari G, Liu S, Sverdlov AL, Ritchie RH, Kemp-Harper BK, Horowitz JD, Chirkov YY. The nitric oxide redox sibling nitroxyl partially circumvents impairment of platelet nitric oxide responsiveness. *Nitric Oxide*. 2013; 35:72–78.

70. Shoman ME, Aly OM. Nitroxyl (HNO): A possible strategy for fighting cancer. *Curr Top Med Chem*. 2016;

71. Orescanin ZS, Milovanovic SR, Spasic SD, Jones DR, Spasic MB. Different responses of mesenteric artery from normotensive and spontaneously hypertensive rats to nitric oxide and its redox congeners. *Pharmacol Rep*. 2007; 59:315–22.

72. Miranda KM, Yamada K, Espey MG, Thomas DD, DeGraff W, Mitchell JB, Krishna MC, Colton CA, Wink DA. Further evidence for distinct reactive intermediates from nitroxyl and peroxynitrite: effects of buffer composition on the chemistry of Angeli's salt and synthetic peroxynitrite. *Arch. Biochem. Biophys.* 2002; 401:134–144.

73. Irvine JC, Favaloro JL, Widdop RE, Kemp-Harper BK. Nitroxyl anion donor, Angeli's salt, does not develop tolerance in rat isolated aortae. *Hypertension*. 2007; 49:885–892.

74. Irvine JC, Kemp-Harper BK, Widdop RE. Chronic administration of the HNO donor Angeli's salt does not lead to tolerance, cross-tolerance, or endothelial dysfunction: comparison with GTN and DEA/NO. *Antioxid. Redox Signal.* 2011; 14:1615–1624.

75. Paolocci N, Saavedra WF, Miranda KM, Martignani C, Isoda T, Hare JM, Espey MG, Fukuto JM, Feelisch M, Wink DA, Kass DA. Nitroxyl anion exerts redox-sensitive positive cardiac inotropy in vivo by calcitonin gene-related peptide signaling. *Proc Natl Acad Sci U S A*. 2001; 98:10463–8.

76. Favaloro JL, Kemp-Harper BK. The nitroxyl anion (HNO) is a potent dilator of rat coronary vasculature. *Cardiovasc Res*. 2007; 73:587–96.

77. Owman C. Peptidergic vasodilator nerves in the peripheral circulation and in the vascular beds of the heart and brain. *Blood Vessels*. 1990; 27:73–93.

78. Edvinsson L, Ekman R, Jansen I, McCulloch J, Mortensen A, Uddman R. Reduced levels of calcitonin gene-related peptide-like immunoreactivity in human brain vessels after subarachnoid haemorrhage. *Neurosci. Lett.* 1991; 121:151–154.

79. DiPette DJ, Schwarzenberger K, Kerr N, Holland OB. Systemic and regional hemodynamic effects of calcitonin gene-related peptide. *Hypertension*. 1987; 9:III142–146.

80. Arumugam TV, Chan SL, Jo DG, Yilmaz G, Tang SC, Cheng A, Gleichmann M, Okun E, Dixit VD, Chigurupati S, Mughal MR, Ouyang X, Miele L, Magnus T, Poosala S, Granger DN, Mattson MP. Gamma secretase-mediated Notch signaling worsens brain damage and functional outcome in ischemic stroke. *Nat Med*. 2006; 12:621–3.

81. Williams JR, Harrison TR, Grollman A. A SIMPLE METHOD FOR DETERMINING THE SYSTOLIC BLOOD PRESSURE OF THE UNANESTHETIZED RAT. *J Clin Invest*. 1939; 18:373–6.

82. Van Nimwegen C, Van Eijnsbergen B, Boter J, Mullink JW. A simple device for indirect measurement of blood pressure in mice. *Lab Anim*. 1973; 7:73–84.

83. Schwedhelm E, Tsikas D, Durand T, Gutzki FM, Guy A, Rossi JC, Frolich JC. Tandem mass spectrometric quantification of 8-iso-prostaglandin F2alpha and its metabolite

2,3-dinor-5,6-dihydro-8-iso-prostaglandin F2alpha in human urine. *J Chromatogr B Biomed Sci Appl*. 2000; 744:99–112.

84. Ellman GL. Tissue sulfhydryl groups. *Arch Biochem Biophys*. 1959; 82:70–7.

85. Van Eck M, Hoekstra M, Hildebrand RB, Yaong Y, Stengel D, Kruijt JK, Sattler W, Tietge UJ, Ninio E, Van Berkel TJ, Pratico D. Increased oxidative stress in scavenger receptor BI knockout mice with dysfunctional HDL. *Arterioscler Thromb Vasc Biol*. 2007; 27:2413–9.

86. Furchgott RF, Zawadzki JV. The obligatory role of endothelial cells in the relaxation of arterial smooth muscle by acetylcholine. *Nature*. 1980; 288:373–6.

87. Zhang SH, Reddick RL, Piedrahita JA, Maeda N. Spontaneous hypercholesterolemia and arterial lesions in mice lacking apolipoprotein E. *Science*. 1992; 258:468–71.

88. Paolocci N, Katori T, Champion HC, St John ME, Miranda KM, Fukuto JM, Wink DA, Kass DA. Positive inotropic and lusitropic effects of HNO/NO- in failing hearts: independence from beta-adrenergic signaling. *Proc Natl Acad Sci U S A*. 2003; 100:5537–42.

89. Archer SL, Huang JM, Hampl V, Nelson DP, Shultz PJ, Weir EK. Nitric oxide and cGMP cause vasorelaxation by activation of a charybdotoxin-sensitive K channel by cGMP-dependent protein kinase. *Proc. Natl. Acad. Sci. U.S.A.* 1994; 91:7583–7587.

90. Garthwaite J, Southam E, Boulton CL, Nielsen EB, Schmidt K, Mayer B. Potent and selective inhibition of nitric oxide-sensitive guanylyl cyclase by 1H-[1,2,4]oxadiazolo[4,3-a]quinoxalin-1-one. *Mol Pharmacol*. 1995; 48:184–8.

91. Wanstall JC, Jeffery TK, Gambino A, Lovren F, Triggle CR. Vascular smooth muscle relaxation mediated by nitric oxide donors: a comparison with acetylcholine, nitric oxide and nitroxyl ion. *Br J Pharmacol*. 2001; 134:463–72.

92. Favaloro JL, Kemp-Harper BK. Redox variants of NO (NO and HNO) elicit vasorelaxation of resistance arteries via distinct mechanisms. *Am J Physiol Heart Circ Physiol*. 2009; 296:H1274–80.

93. Haynes J, Robinson J, Saunders L, Taylor AE, Strada SJ. Role of cAMP-dependent protein kinase in cAMP-mediated vasodilation. *Am. J. Physiol.* 1992; 262:H511–516.

94. Morello S, Vellecco V, Alfieri A, Mascolo N, Cicala C. Vasorelaxant effect of the flavonoid galangin on isolated rat thoracic aorta. *Life Sci.* 2006; 78:825–830.

95. Fabbri E, Brighenti L, Ottolenghi C. Inhibition of adenylate cyclase of catfish and rat hepatocyte membranes by 9-(tetrahydro-2-furyl)adenine (SQ 22536). *J Enzyme Inhib*. 1991; 5:87–98.

96. Brayden JE. Potassium channels in vascular smooth muscle. *Clin Exp Pharmacol Physiol*. 1996; 23:1069–76.

97. Lenaeus MJ, Vamvouka M, Focia PJ, Gross A. Structural basis of TEA blockade in a model potassium channel. *Nat Struct Mol Biol*. 2005; 12:454–9.

98. Tricarico D, Camerino DC. ATP-sensitive K+ channels of skeletal muscle fibers from young adult and aged rats: possible involvement of thiol-dependent redox mechanisms in the age-related modifications of their biophysical and pharmacological properties. *Mol Pharmacol*. 1994; 46:754–61.

99. Cole WC. Silencing vascular smooth muscle ATP-sensitive K+ channels with caveolin-1. *J Physiol*. 2010; 588:3133–4.

100. Beck-Nielsen H, Hother-Nielsen O, Pedersen O. Mechanism of action of sulphonylureas with special reference to the extrapancreatic effect: an overview. *Diabet Med*. 1988; 5:613–20.

101. Wang ZW, Nara M, Wang YX, Kotlikoff MI. Redox regulation of large conductance Ca(2+)-activated K+ channels in smooth muscle cells. *J Gen Physiol*. 1997; 110:35–44.

102. Galvez A, Gimenez-Gallego G, Reuben JP, Roy-Contancin L, Feigenbaum P, Kaczorowski GJ, Garcia ML. Purification and characterization of a unique, potent, peptidyl probe for the high conductance calcium-activated potassium channel from venom of the scorpion Buthus tamulus. *J Biol Chem*. 1990; 265:11083–90.

103. Wang G, Strang C, Pfaffinger PJ, Covarrubias M. Zn2+-dependent redox switch in the intracellular T1-T1 interface of a Kv channel. *J Biol Chem*. 2007; 282:13637–47.

104. Gillespie JI, Hutter OF. Proceedings: The actions of 4-aminopyridine on the delayed potassium current in skeletal muscle fibres. *J Physiol*. 1975; 252:70P–71P.

105. Gardiner SM, Compton AM, Bennett T. Regional haemodynamic effects of human alpha- and beta-calcitonin gene-related peptide in conscious Wistar rats. *Br J Pharmacol*. 1989; 98:1225–32.

106. Arnold WP, Mittal CK, Katsuki S, Murad F. Nitric oxide activates guanylate cyclase and increases guanosine 3':5'-cyclic monophosphate levels in various tissue preparations. *Proc Natl Acad Sci U S A*. 1977; 74:3203–7.

107. Lopez BE, Shinyashiki M, Han TH, Fukuto JM. Antioxidant actions of nitroxyl (HNO). *Free Radic Biol Med*. 2007; 42:482–91.

108. Carmichael ST. Rodent models of focal stroke: size, mechanism, and purpose. *NeuroRx*. 2005; 2:396–409.

109. Durukan A, Tatlisumak T. Acute ischemic stroke: overview of major experimental rodent models, pathophysiology, and therapy of focal cerebral ischemia. *Pharmacol. Biochem. Behav.* 2007; 87:179–197.

110. Shivakumar BR, Kolluri SV, Ravindranath V. Glutathione and protein thiol homeostasis in brain during reperfusion after cerebral ischemia. *J. Pharmacol. Exp. Ther.* 1995; 274:1167–1173.

111. Shih AY, Li P, Murphy TH. A small-molecule-inducible Nrf2-mediated antioxidant response provides effective prophylaxis against cerebral ischemia in vivo. *J. Neurosci.* 2005; 25:10321–10335.

112. Simoni RD, Hill RL, Vaughan M. On glutathione. II. A thermostable oxidation-reduction system (Hopkins, F. G., and Dixon, M. (1922) J. Biol. Chem. 54, 527-563). *J Biol Chem*. 2002; 277:e13.

113. Jin G, Tsuji K, Xing C, Yang Y-G, Wang X, Lo EH. CD47 gene knockout protects against transient focal cerebral ischemia in mice. *Exp. Neurol.* 2009; 217:165–170.

114. Ma XL, Gao F, Liu GL, Lopez BL, Christopher TA, Fukuto JM, Wink DA, Feelisch M. Opposite effects of nitric oxide and nitroxyl on postischemic myocardial injury. *Proc Natl Acad Sci U S A*. 1999; 96:14617–22.

115. Jusufovic M, Mishra NK, Lansberg MG, Bath PM, Berge E, Sandset EC. Blood pressure management in acute stroke. *Curr Hypertens Rev*. 2016;

116. Leo CH, Joshi A, Hart JL, Woodman OL. Endothelium-dependent nitroxyl-mediated relaxation is resistant to superoxide anion scavenging and preserved in diabetic rat aorta. *Pharmacol. Res.* 2012; 66:383–391.

117. Nagaraja TN, Karki K, Ewing JR, Croxen RL, Knight RA. Identification of variations in blood-brain barrier opening after cerebral ischemia by dual contrast-enhanced magnetic resonance imaging and T 1sat measurements. *Stroke*. 2008; 39:427–32.

118. Abulrob A, Brunette E, Slinn J, Baumann E, Stanimirovic D. Dynamic analysis of the blood-brain barrier disruption in experimental stroke using time domain in vivo fluorescence imaging. *Mol Imaging*. 2008; 7:248–262.

119. Zeller A, Wenzl MV, Beretta M, Stessel H, Russwurm M, Koesling D, Schmidt K, Mayer B. Mechanisms underlying activation of soluble guanylate cyclase by the nitroxyl donor Angeli's salt. *Mol Pharmacol*. 2009; 76:1115–22.

120. Shieh CC, Coghlan M, Sullivan JP, Gopalakrishnan M. Potassium channels: molecular defects, diseases, and therapeutic opportunities. *Pharmacol Rev*. 2000; 52:557–94.

121. Toro L, Vaca L, Stefani E. Calcium-activated potassium channels from coronary smooth muscle reconstituted in lipid bilayers. *Am J Physiol*. 1991; 260:H1779–89.

122. Fisher M. New approaches to neuroprotective drug development. *Stroke*. 2011; 42:S24–7.

123. Fisher M, Feuerstein G, Howells DW, Hurn PD, Kent TA, Savitz SI, Lo EH. Update of the stroke therapy academic industry roundtable preclinical recommendations. *Stroke*. 2009; 40:2244–50.

124. Dittmar MS, Vatankhah B, Fehm NP, Schuierer G, Bogdahn U, Horn M, Schlachetzki F. Fischer-344 rats are unsuitable for the MCAO filament model due to their cerebrovascular anatomy. *J Neurosci Methods*. 2006; 156:50–4.

125. Song WL, Lawson JA, Reilly D, Rokach J, Chang CT, Giasson B, FitzGerald GA. Neurofurans, novel indices of oxidant stress derived from docosahexaenoic acid. *J Biol Chem*. 2008; 283:6–16.

126. Donzelli S, Fischer G, King BS, Niemann C, DuMond JF, Heeren J, Wieboldt H, Baldus S, Gerloff C, Eschenhagen T, Carrier L, Böger RH, Espey MG. Pharmacological characterization of 1-nitrosocyclohexyl acetate, a long-acting nitroxyl donor that shows vasorelaxant and antiaggregatory effects. *J. Pharmacol. Exp. Ther.* 2013; 344:339–347.

8 Acknowledgments

Ich möchte mich bei meinem Doktorvater Prof. Dr. med. Rainer H. Böger, Direktor des Instituts für Klinische Pharmakologie und Toxikologie bedanken, der mir die Möglichkeit gab diese Doktorarbeit in seinem Institut und unter seiner Leitung durchzuführen. Er führte mich hart aber stets fair. Retrospektiv bin ich über jede seiner kritischen Anmerkungen sehr dankbar.

Dank gilt zudem Prof. Dr. med. Christian Gerloff und Dr. med. Chi-un Choe aus der Klinik für Neurologie, die bei den Mäusen die Schlaganfälle induzierten und mir Blut- und Urinproben zum analytischen Teil dieser Doktorarbeit zur Verfügung stellten.

Ferner bedanke ich mich bei Dr. med. Munif Haddad, ehemals Instituts für Klinische Chemie, der keine Sekunde zögerte und mir seine Laborstraße und sein Team zur Kreatininmessung im Mausurin zur Verfügung stellte.

Dank gebührt zudem, PD Dr. rer. nat. Edzard Schwedhelm, Dr. rer. nat. Gregor Sachse, Anna Steenpaß, Mariola Kastner, Cornelia Woermann und all den anderen im Institut für Klinische Pharmakologie und Toxikologie dafür, dass sie mich in die Methodik eingearbeitet und auch sonst meine Launen ertragen haben. Dank auch an Daniel für das Korrekturlesen.

Besonders möchte ich mich bei Sonia Donzelli, PhD bedanken, die mir immer den Rücken freigehalten hat und mir völlige Freiheit in der Planung und Durchführung der Experimente gewährte. Dein Tiramisu ist das Beste!

Ich möchte mich bei meinen Freunden, besonders bei Georg und Gunnar bedanken.

Letztlich möchte ich mich bei meinen Eltern bedanken, die immer für mich da waren und sind.

9 Curriculum Vitae

Entfällt aus datenschutzrechtlichen Gründen.

10 Statutory declaration

Ich versichere ausdrücklich, dass ich die Arbeit selbständig und ohne fremde Hilfe verfasst, andere als die von mir angegebenen Quellen und Hilfsmittel nicht benutzt und die aus den benutzten Werken wörtlich oder inhaltlich entnommenen Stellen einzeln nach Ausgabe (Auflage und Jahr des Erscheinens), Band und Seite des benutzten Werkes kenntlich gemacht habe.
Ferner versichere ich, dass ich die Dissertation bisher nicht einem Fachvertreter an einer anderen Hochschule zur Überprüfung vorgelegt oder mich anderweitig um Zulassung zur Promotion beworben habe.
Ich erkläre mich einverstanden, dass meine Dissertation vom Dekanat der Medizinischen Fakultät mit einer gängigen Software zur Erkennung von Plagiaten überprüft werden kann.

Unterschrift: 

Gerryansjah Fischer